

## **REPORT ON:**

### **MIXED MONOLAYER FILMS OF A SATURATED AND AN UNSATURATED POLAR LIPID. (STEARIC ACID-OLEIC ACID AND DPPC-POPC)**

Juan Torrent-Burgués

Department of Chemical Engineering

Universitat Politècnica de Catalunya

## Contents

### Brief report

- Objective
- Abstract
- Introduction. Bibliographic revision.
- Results and discussion
  - o Stearic acid, oleic acid
  - o DPPC, POPC
- Conclusions
- References

### Full report

- Materials and methods
- Results and discussion
  - o Stearic acid, oleic acid
  - o DPPC, POPC
- Conclusions
- References

## Brief Report

### Objective

- Study the differences in behavior of mixed films of saturated-unsaturated fatty acids as SA-OA vs saturated-unsaturated phospholipids as DPPC-POPC. Using Langmuir,  $\Pi$ -A isotherms, compressibility, excess area, AFM
  - o Influence of the subphase, velocity of compression.
  - o Miscibility of the components
  - o Application of the state equations to describe the individual lipids and their mixtures.

### Abstract

Mixed fatty acids or mixed phospholipids with saturated-unsaturated chains are of biological interest. In this work, the mixtures of oleic acid-stearic acid (OA-SA) and POPC-DPPC have been studied. From the surface pressure-area isotherms, the elastic modulus values and the virial equation coefficients can be obtained. The thermodynamic treatment also allows obtaining the excess and the mixing free energies. Results indicate that molecular interactions in the mixture are less favourable, due to the presence of the unsaturation, but the mixture is slightly favourable due to the entropic factor. For the OA-SA mixture, a high SA content and a high surface pressure facilitate the phase separation, even a certain miscibility between both components still remains. For the POPC-DPPC mixture, the more favourable mixing conditions occurs for  $X_{\text{POPC}} \approx 0.4$ . For these mixtures, the values of the elastic modulus are more similar to those of the more fluid component (OA or POPC) and the analysis of the virial coefficients shows that the  $b_1$  virial coefficient values lies between those of the individual components and higher than those values for an ideal mixing.

### INTRODUCTION

Fatty acids and phospholipids have been widely studied with the Langmuir technique because they are amphiphilic compounds ideal to form ordered and compact monolayers and of their biological interest. Bibliographic references to previous studies can be found in Ulman 1990, Petty 1996, Richardson 2000. Recent articles on simple (single) fatty acids or related amphiphiles are those of Baba 2013, Barzyk 2011, Dhathathreya 2008, Dupres 2003, Kundu 2011, Mildner 2012, Maheshwari 2004, Snow 2014, Yang 2010. Recent articles on single phospholipids are those of Baba 2014, Flasiński 2014, Kaviratna 2009, Rodriguez 2008, Weiss 2008.

As in biological systems mixtures of fatty acids or phospholipids are found, the study of such mixtures is more interesting. Recent articles on mixtures of fatty acids are those of Broniatowski 2006, Brzozowska 2013, Eftaiha 2012a, Imae 2000, Matsumoto 2003,

Matsumoto 2004, Qaqish 2008, Watanabe 2011. Furthermore, as usually fatty acids or phospholipids present unsaturations in the hydrocarbon chains, the study of mixtures of saturated and unsaturated compounds is of interest. Recent articles on mixed saturated-unsaturated fatty acids are those of Ocko 2002, Seoane 2001, and on mixed saturated-unsaturated phospholipids are those of Domenech 2005, Domenech 2006, Dynarowicz 2013, Garcia-Manyes 2007, Ohki 2010, Park 2009, Stefaniu 2014, Wydro 2013a,b, Wydro 2009.

Even the extended literature in the field, no recent articles in the study in deep of stearic acid and oleic acid mixtures or DPPC-POPC mixtures have been reported. In this work these mixtures have been studied using the  $\Pi$ -A isotherms. The thermodynamic behavior of the mixtures has been analyzed through the excess area, the elastic modulus and the state equations.

## RESULTS AND DISCUSSION

### Results

#### A) SA-OA mixture

The isotherms  $\Pi$ -A for the mixtures de SA and OA, together to those of the individual components, are shown in Fig. 1, and in Fig. 2 the values of mean area are plot vs the molar fraction at several surface pressures.

Mixed monolayers shows a first collapse that practically coincides with that of OA ( $\Pi=30$  mN/m), and when the proportion of SA increases, a second collapse is observed which does not reach the value observed for SA ( $\Pi=58$  mN/m). This is an indication that at high surfaces pressures OA forms a separated phase, from SA, which collapses at its surface pressure (30 mN/m), meanwhile the collapse of the SA phase is influenced by the presence of OA, doing the OA molecules a distorting effect on the compactness of the SA molecules to form a more rigid film.

A study of the mean area per molecule (Fig 2) shows positive deviations from the straight line, being these deviations more important at low surface pressures and when the OA content is  $X=0.425$ . At high surface pressures and all compositions except for the OA content of  $X=0.425$ , the mean area gets closer to the straight line. Positive deviations indicate mixing but with unfavorable interactions in respect to pure components. Null deviations indicate ideal mixing or phase separation. As two collapses can be observed in the isotherms when the SA is in great proportion, it indicates that a phase separation occurs then. As experimental points are not on the straight line, it means that a partial miscibility still exists. On the other hand, AFM images (see Full report) of SA-OA LB films transferred on mica show the presence of domains, which can be attributed to separated phases of the components. (The analysis of the area domains in the AFM images also indicates that a certain partial miscibility occurs)

Fig 3 presents the variation of the elastic modulus (eq. 1) along the isotherm compression for the different mixtures of SA and OA.

$$C_s^{-1} = -A \left( \frac{d\pi}{dA} \right)_T$$

(eq. 1)

Mixtures show a LE state, but when the SA content is high, a LC state appears at higher surface pressures.

It is also seen that when the SA content increases, the surface pressure at the inflexion point in the isotherm, or at the first maximum point in the compressibility plot, decreases. By the contrary the second maximum point in the compressibility plot increases with the SA content.

These results also point to a partial mixing at low surface pressures but a segregation at high surface pressures, especially at high SA content.

For the isotherms of SA-OA mixtures, a study dealing with state equations has also been done. For this study, the virial state equation (eq. 2) has been applied.

$$\Pi A/(kT) = b_0 + b_1 \Pi + b_2 \Pi^2, \quad (\text{eq. 2})$$

where  $b_0$ ,  $b_1$  and  $b_2$  are the virial coefficients.

Fig. 4 shows the plots of  $(\Pi A/kT)$  vs  $\Pi$  for the several studied compositions, which can be adjusted with a polynomial of 2<sup>nd</sup> degree,

The values of the virial coefficients are tabulated in table 1.

The following treatment can be applied to the mixture virial coefficients.

$$- \quad b_{1m} = b_{11}X_1^2 + b_{12}X_2^2 + 2b_{112}X_1X_2 \quad (\text{eq. 3.1})$$

$$- \quad b_{1m}^{id} = b_{11}X_1 + b_{12}X_2 \quad (\text{eq. 3.2})$$

$$- \quad b_{1E} = b_{1m} - b_{1m}^{id} \quad (\text{eq. 3.3})$$

The values of  $b_{112}$  and  $b_{1E}$  are tabulated in Table 2 .

Results for  $b_1$  coef (Fig 15) indicate a gradual decrease from the OA to the SA. Similar occurs for the  $b_0$  coef. The higher value for  $b_1$  of OA is due to the higher repulsive interactions between molecules in this fatty acid in respect to the SA. The higher value for  $b_0$  of OA is due to a less degree of aggregation in this fatty acid in respect to the SA. The values of  $b_{1m}$  are in between those of the SA and OA, but higher than those of the straight line, that is the  $b_{1E}$  values are positive. This indicates more repulsive interactions in the mixture between SA and OA molecules, in respect to the separate components.

The values of  $b_{112}$  are positive and higher than the mean value  $(b_{11} + b_{12})/2 = 0.09105$ , which also indicates more repulsion in the mixture between molecules.

The higher values of  $b_1^{12}$  occurs when the content of OA is low, being higher than the value of  $b_1$  of pure OA. This fact can be explained because OA breaks the compactness of SA which results in an increase of the  $b_1$  coefficient (much more repulsion in respect to pure components).

As positive deviations are higher for low  $X(\text{OA})$ , it means that OA places partially in between SA, destabilizing the compactness of SA. When there is low SA content it can better mix with the fluid phase of OA and the interactions are less unfavorable, and the positive deviations are lower. Thus, the domain formation or phase separation could be more notable for low  $X(\text{OA})$ .

**Table 1**

Virial coef	OA	80:20	60:40	40:60	20:80	SA
<b>B0</b>	<b>0.0055</b>	<b>0.0050</b>	<b>0.0046</b>	<b>0.0048</b>	<b>0.0007</b>	<b>-0.0021</b>
<b>B1</b>	<b>0.1255</b>	<b>0.1208</b>	<b>0.1080</b>	<b>0.1064</b>	<b>0.0883</b>	<b>0.0566</b>
<b>B2</b>	<b>-0.0015</b>	<b>-0.0015</b>	<b>-0.0014</b>	<b>-0.0013</b>	<b>-0.0011</b>	<b>-0.00018</b>
<b>R2</b>	<b>0.9994</b>	<b>0.9994</b>	<b>0.9994</b>	<b>0.9997</b>	<b>0.9999</b>	<b>0.9974</b>

**Table 2**

$X(\text{OA})$	$b_1$	$b_1^{12}$	$b_1^E$
0	0,0566		0
0,217	0,0883	0,14033669	0,0167487
0,425	0,1064	0,13302954	0,0205175
0,625	0,108	0,10883667	0,0083375
0,816	0,1208	0,1176165	0,0079776
1	0,1255		0

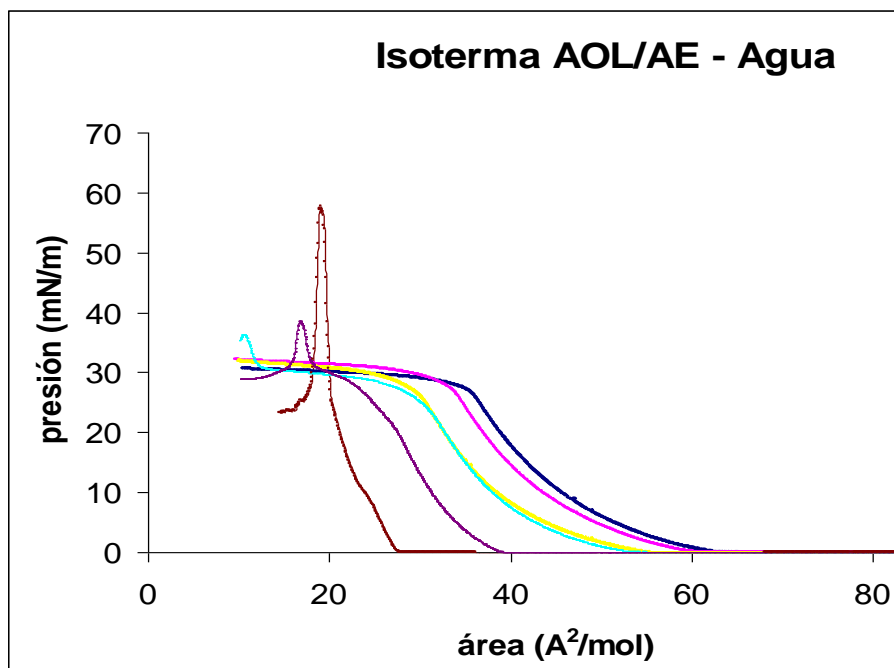


Figure 1. Isotherms for mixtures of OA+SA. Blue) OA, magenta) 80:20, yellow) 60:40, cyan) 40:60, violet) 20:80, brown) SA. Area represents the mean area per molecule.

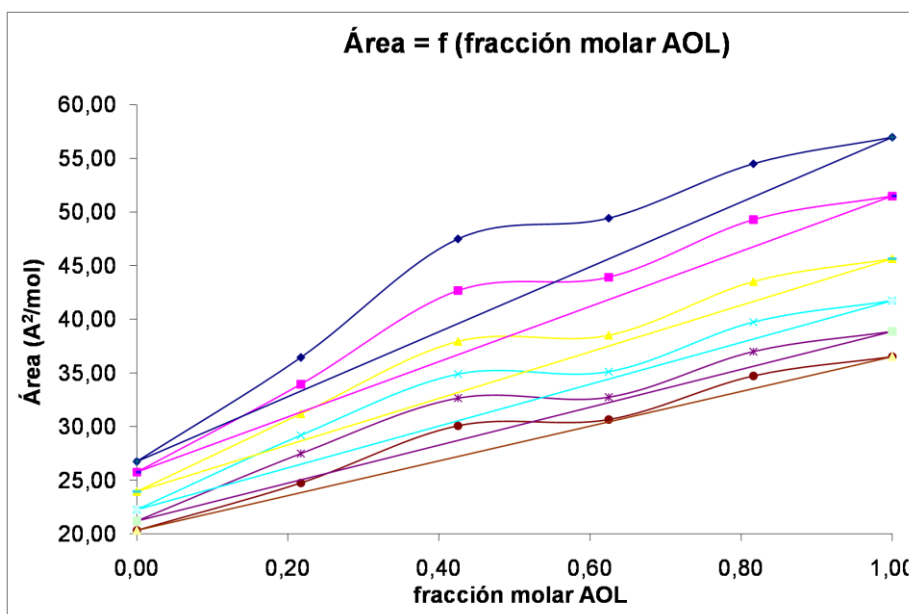


Figure 2. Area vs composition for mixtures OA+SA, at different surface pressures: blue) 2, magenta) 5, yellow) 10, cyan) 15, violet) 20, brown) 25 mN/m.

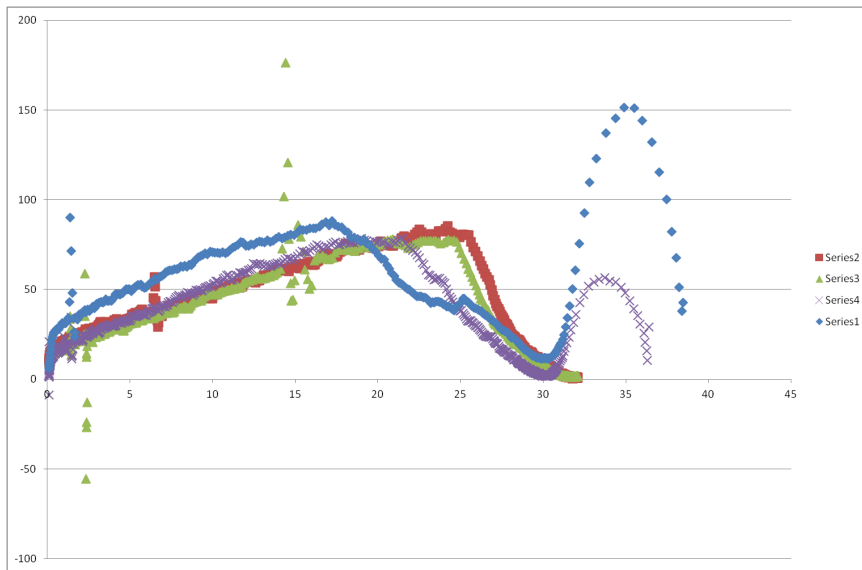
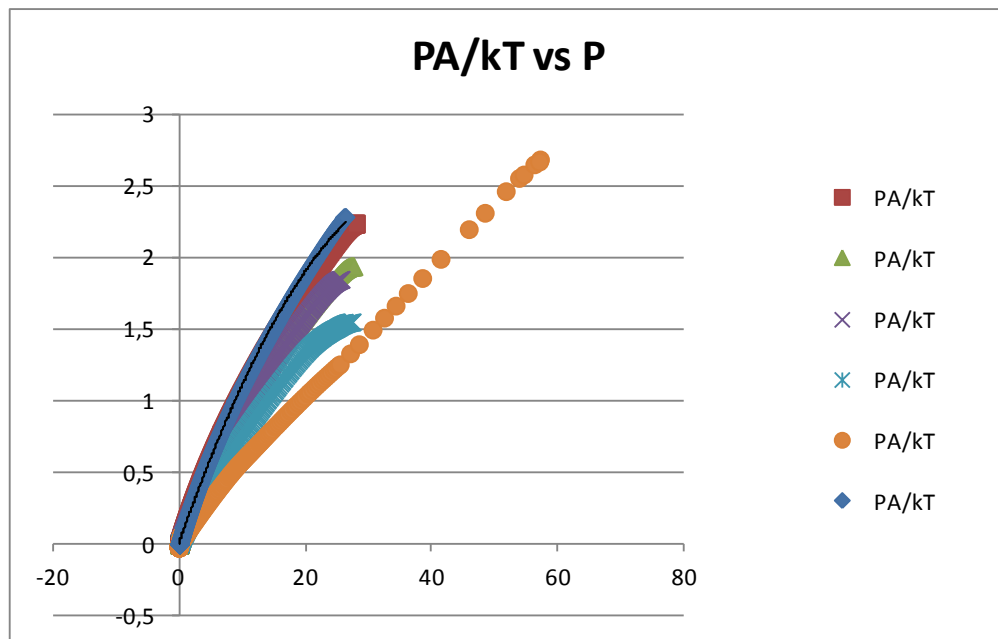


Fig 3. Elastic modulus. Mixtures OA:SA, 80:20 (brown), 60:40 (green), 40:60 (violet), 20:80 (blue).

Fig 4a. plots of  $(\Pi A/kT)$  vs  $\Pi$  for the several studied compositions. (mixture + individuals)



blue: oleic

yellow:  
estearic

red 80:20    green 60:40    violet 40:60    cyan 20:80

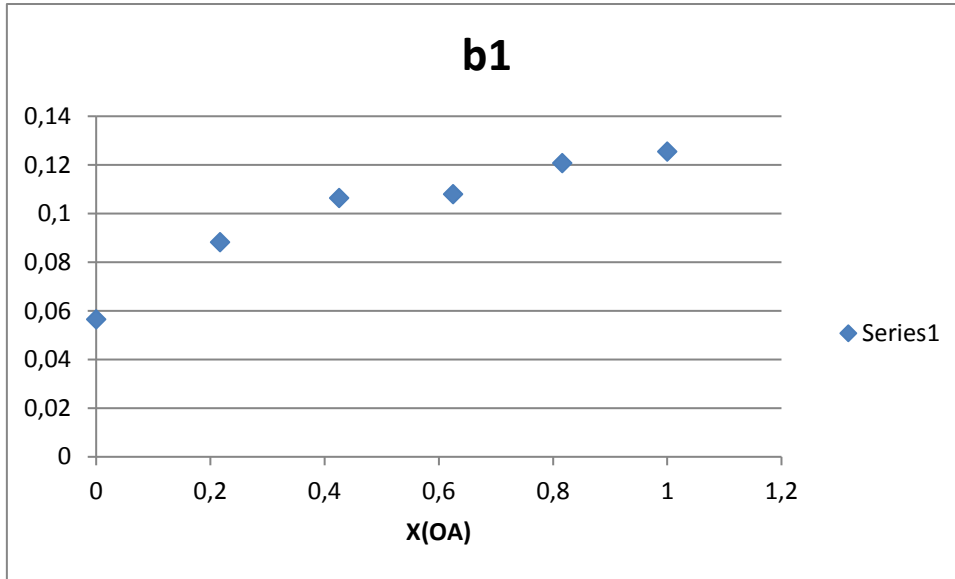


Fig 4b. Values of  $b_1$  for mixtures of OA and SA.

#### B) DPPC-POPC mixture

Fig. 5 shows the  $\Pi$ -A isotherms of mixtures of DPPC and POPC, together with those of the individual components. It is observed that the phase change of DPPC at  $\Pi=8$  mN/m is influenced by the presence of POPC, as well as the collapse pressure, indicating that DPPC and POPC mix in a certain degree.

Fig 6 shows the mean area per molecule vs the POPC molar fraction, at several  $\Pi$ . It is observed in general positive deviations respect to the ideal case (straight line), but at low and high P the mixture with  $X(\text{POPC})=0.4$  present negative deviations which indicate less repulsive interactions or more attractive interactions (favorable interactions in respect to the individual components). In both cases, deviations from the straight line indicate a certain degree of miscibility. This fact will be commented later.

Fig 7 shows the inverse of the compressibility coefficient (the elastic modulus) of DPPC, POPC and DPPC-POPC mixtures, obtained from the isotherms of Fig 5 using the equation 1. DPPC presents a phase change from LE to LC at P around 8 mN/m, and POPC only presents LE state. Mixtures DPPC-POPC studied only presents LE state, with an inflexion at high DPPC contents, with the inflexion Pressure increasing when the DPPC content decreases.

An analysis of the isotherms using the virial state equation has been done.

The plot of  $\Pi A/(kT)$  vs  $\Pi$  (Fig 8a) can be adjusted with a polynomial de 2n degree (eq 2),  $\Pi A/(kT)=b_0+b_1\Pi+b_2\Pi^2$ , where  $b_0$ ,  $b_1$  and  $b_2$  are the virial coefficients, and the same treatment reported in eq (3) is now applied to them.



The values of the viral coefficients are tabulated in table 3 and the values of  $b_1$  and  $b_{12}$  are tabulated in Table 4.

Table 3.

Virial coef	POPC	POPC 80	POPC 60	POPC 40	POPC 20	DPPC
B0	0.0319	0.0856	0.0923	0.0832	0.0978	0.1930
B1	0.2002	0.1991	0.1984	0.1744	0.1736	0.1333
B2	-0.0017	-0.0016	-0.0019	-0.0016	-0.0016	-0.00068
R2	0.9994	0.9995	0.9992	0.9989	0.9970	0.9916

**Table 4**

X(POPC)	$b_1$	$b_{12}$	$b_{1E}$
0	0,1333		0
0,191	0,1736	0,256	0,0275
0,394	0,1744	0,198	0,0147
0,596	0,1984	0,219	0,0252
0,798	0,1991	0,205	0,0124
1	0,2002		0

It is seen from the table that  $b_1$  increases with the POPC content. This indicates more repulsive interactions for POPC and that the presence of POPC in the DPPC matrix also increases the repulsive interactions between molecules, in respect to DPPC molecules. The value of  $b_0$  for POPC is lower than that of DPPC, indicating more aggregation in POPC than in DPPC (even POPC has an unsaturation, the oleoil chain is larger. Another explanation could be in the phase change of DPPC that makes the linear fit more problematic).

Results for  $b_1$  coef (Fig 8b) indicate a gradual decrease from the POPC to the DPPC. The higher value for  $b_1$  of POPC is due to the higher repulsive interactions between molecules in this fatty acid in respect to the DPPC. The values of  $b_{1m}$  are in between those of the DPPC and POPC, but higher than those of the straight line, that is the  $b_{1E}$  values are positive. This indicates more repulsive interactions in the mixture between DPPC and POPC molecules, in respect to the separate components. The values of  $b_{12}$  are positive and higher than the mean value  $(b_1 + b_2)/2 = 0.1667$ , which also indicates more repulsion in the mixture between molecules.

The higher values of  $b_{12}$  occurs when the content of POPC is low, being higher than the value of  $b_1$  of pure POPC, except that of  $X(\text{POPC})=0.4$ . This fact can be explained because POPC breaks the compactness of DPPC which results in an increase of the  $b_1$  coefficient (much more repulsion in respect to pure components). As has been seen previously, when  $X(\text{POPC})=0.4$  the excess area is negative which is in agreement with the fact that seen now that the  $b_{12}$  is the low value for the mixture and being lower than that of pure POPC. Thus, the mixture with  $X(\text{POPC})=0.4$  is the most favorable of the mixtures.

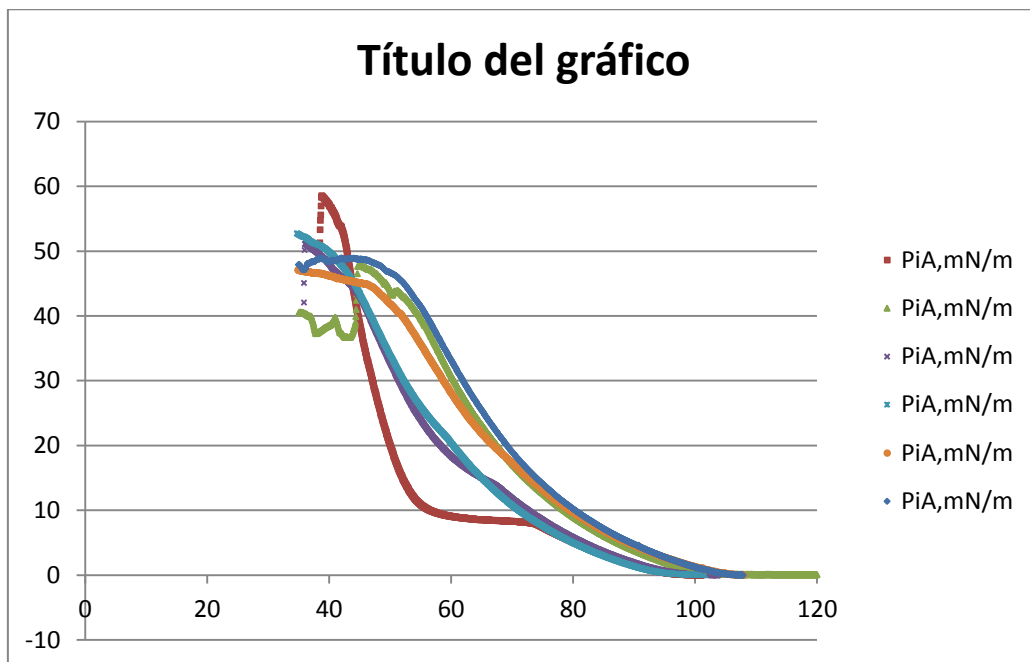
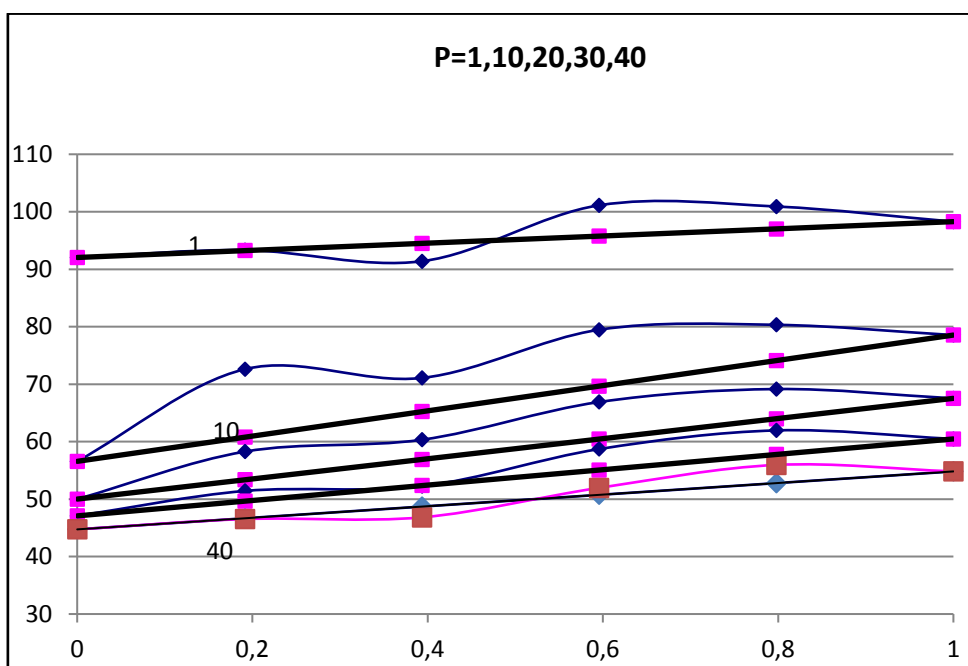


Fig 5.  $\Pi$ -A isotherms of DPPC, POPC and DPPC-POPC mixtures. Colors: brown) DPPC, etc, blue) POPC.



**Fig 6.** Area vs composition in mixtures DPPC+POPC, at different surface pressures: 1, 10, 20, 30, 40 mN/m.

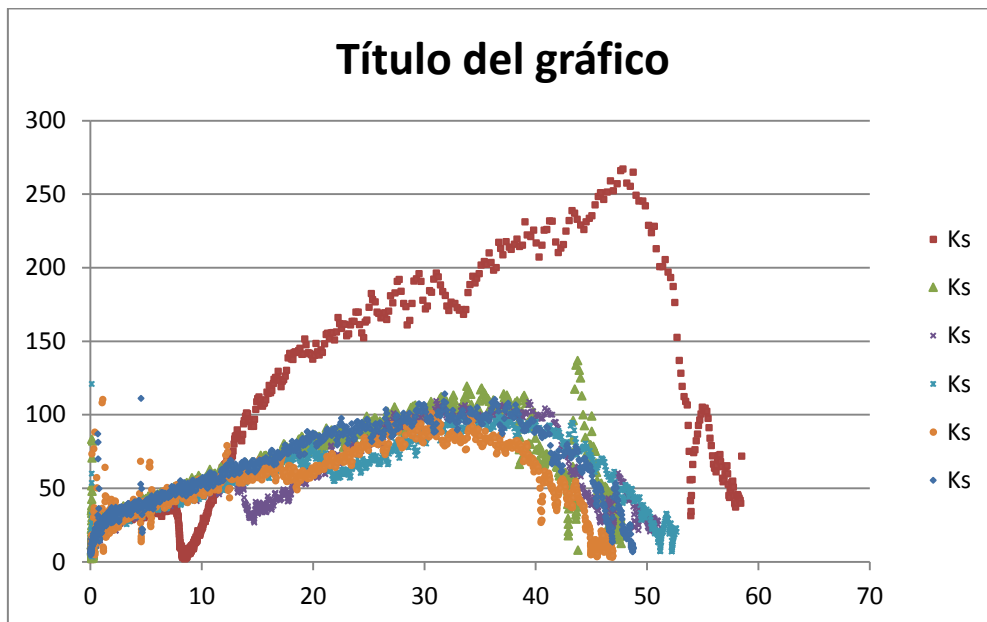


Fig 7. Elastic modulus of DPPC, POPC and DPPC-POPC mixtures. Colors: brown) DPPC etc, blue) POPC.

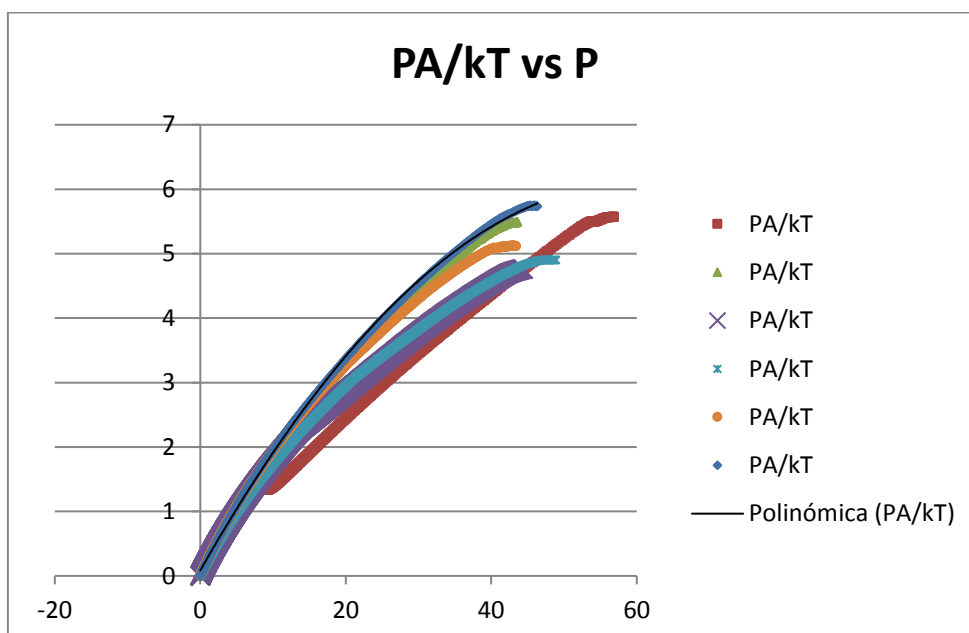


Fig 8a. Plots of  $(\Pi A/kT)$  vs  $\Pi$  for the several studied compositions. (Mixture + individuals)

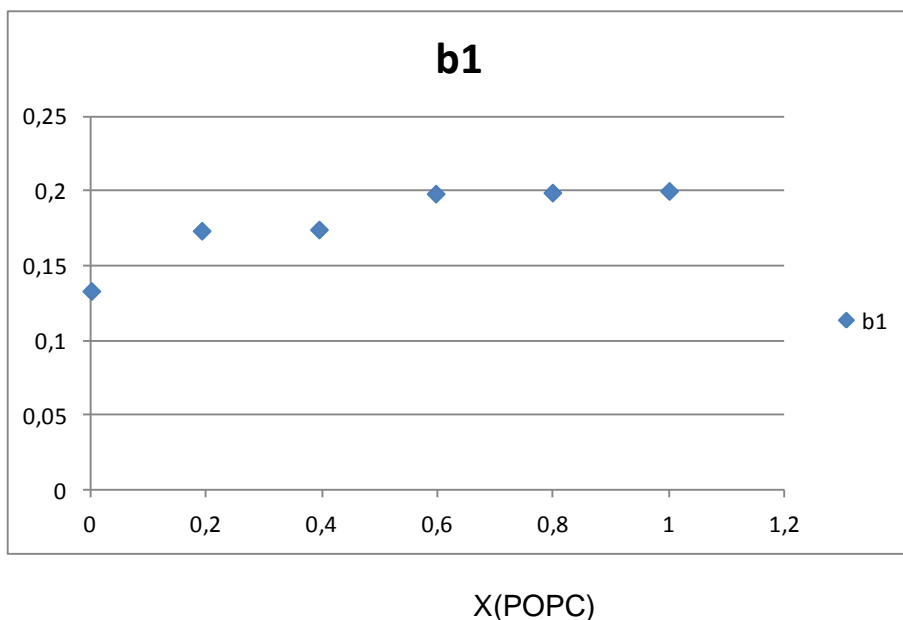


Fig 8b. Values of  $b_1$  for mixtures of DPPC and POPC.

## Discussion

Isotherms indicate that certain miscibility between components can be present in both cases, SA-OA and DPPC-POPC, but it will be more important for the phospholipids than for the fatty acids. The  $A$  vs  $X$  analysis shows this effect of miscibility but with less favorable interactions in respect to the individual components. Thus, the miscibility should be attributed to entropic factors. The less favorable interactions lead to the partial phase segregation that is observed (in isotherms and AFM images) for the SA-OA system at high pressures and/or at high SA content. For the DPPC-POPC system there is a composition ( $X(\text{POPC})=0.4$ ) where the mixture is favourable.

The less favourable interactions could be due, at least in part, to the presence of the insaturation.

The values of the compressibility coefficients likes more to those of the more fluid component (OA or POPC). The behavior of the compressibility curves at high surface pressures is different comparing both systems. The DPPC-POPC system presents only one maximum, meanwhile the OA-SA system presents two maxima with a clear phase with SA for the second maximum.

The analysis of the virial coefficients is similar in both systems, with the  $b_1$  values between those of the individual components.

A notable difference between both systems is that meanwhile the OA-SA system at  $X(\text{OA})=0.4$  presents less favourable interactions, the POPC-DPPC system presents at  $X(\text{POPC})=0.4$  more favourable interactions.

## CONCLUSIONS

The presence of an unsaturation in the aliphatic chain of a fatty acid, e.g. oleic acid, or a phospholipid, e.g. POPC, in a mixed film with a saturated one, e.g. stearic acid or DPPC, respectively, makes the molecular interaction less favourable and the excess free energy takes positive values. Nevertheless, the entropic factor leads to slightly negative values of the mixing free energy. This situation facilitates the phase separation (even partial mixing remains), especially at high content of the saturated lipid and high surface pressures, since the saturated lipid tends to a more compact state. For the OA-SA mixture the most favourable mixing situation occurs at  $X_{\text{OA}} \approx 0.6$  meanwhile for the POPC-DPPC it occurs at  $X_{\text{POPC}} \approx 0.4$ . The second virial coefficient  $b_1$  for the mixtures takes values in between those of the individual components but above that of an ideal mixing. The elastic modulus behaviour for the mixtures gets closer to the unsaturated component. For the POPC-DPPC mixtures, these are always in the LE state, similarly to POPC, meanwhile for the OA-SA mixtures a LC state forms at high SA content and high surface pressures, probably due to the phase separation induced by SA.

## REFERENCES

Baba et al (Teruhiko Baba, Katsuki Takai, Toshiyuki Takagi, Toshiyuki Kanamori, *Chemistry and Physics of Lipids* 172– 173 (2013) 31– 39. Effect of perfluoroalkyl chain length on monolayer behavior of partially fluorinated oleic acid molecules at the air–water interface.

Baba et al (Teruhiko Baba, Katsuki Takai, Toshiyuki Takagi, Toshiyuki Kanamori. *Colloids and Surfaces B: Biointerfaces* 123 (2014) 246–253. Effect of the fluorination degree of hydrophobic chains on the monolayer behavior of unsaturated diacylphosphatidylcholines bearing partially fluorinated 9-octadecynoyl (stearoloyl) groups at the air–water interface.

Barzyk and Vuorinen (W Barzyk, J Vuorinen, *Colloids Surf A* 385 (2011) 1-10. Application of the vibrating plate technique to measuring electric surface potential,  $\Delta V$ , of solutions; the flow cell for simultaneous measurement of the  $\Delta V$  and the surface pressure.

Broniatowski and Dynarowicz-Latka (M Broniatowski and P Dynarowicz-Latka, *Langmuir* 22 (2006) 2691-2696. Semifluorinated chains at the air/water interface: studies of the interaction of a semifluorinated alkane with fluorinated alcohols in mixed Langmuir monolayers.

Brzozowska et al (A.M. Brzozowska, F. Mugele, M.H.G. Duits, *Colloids and Surfaces A: Physicochem. Eng. Aspects* 433 (2013) 200– 211. Stability and interactions in mixed monolayers of fatty acid derivatives on Artificial Sea Water.

Dhathathreyan (A Dhathathreyan, *Colloids Surf A* 318 (2008) 307-314. Dissociation constants of long-chain hydroxy fatty acids in Langmuir-Blodgett films.

Dynarowicz-Łatka et al (Patrycja Dynarowicz-Łatka, Anita Wnetrzak, Marcin Broniatowski, Michał Flasiński, *Colloids and Surfaces B: Biointerfaces* 107 (2013) 43– 52. Miscibility and phase separation in mixed erucylphosphocholine–DPPC Monolayers.

Domenech et al (Nos COLSUB 2005) POPE-POPC.

Domenech et al (Òscar Domènech, Fausto Sanz, M. Teresa Montero, Jordi Hernández-Borrell, *Biochimica et Biophysica Acta* 1758 (2006) 213–221. Thermodynamic and structural study of the main phospholipid components comprising the mitochondrial inner membrane.

Dupres et al (V Dupres, S Cantin, F Benhabib, F Perrot, P Fontaine, M Goldmann, J Daillant, O Konovalov, *Langmuir* 19 (2003) 10808-10815. Superlattice formation in fatty acid monolayers on a divalent ion subphase: Role of chain length, temperature, and subphase concentration.

Eftaiha and Paige (A F. Eftaiha, M F. Paige, *Journal of Colloid and Interface Science* 380 (2012a) 105–112. Phase-separation of mixed surfactant monolayers: A comparison of film morphology at the solid–air and liquid–air interfaces.

Flasinski et al (Michał Flasinski, Paweł Wydro, Marcin Broniatowski, [Journal of Colloid and Interface Science](#) 418 (2014) 20–30. Lyso-phosphatidylcholines in Langmuir monolayers – Influence of chain length on physicochemical characteristics of single-chained lipids.

Garcia-manyes et al (Sergi Garcia-Manyes, Òscar Domènech, Fausto Sanz, M.Teresa Montero, Jordi Hernandez-Borrell, *Biochimica et Biophysica Acta* 1768 (2007) 1190–1198. Atomic force microscopy and force spectroscopy study of Langmuir–Blodgett films formed by heteroacid phospholipids of biological interest.

Imae et al (T Imae, T Takeshita, M Kato, *Langmuir* 16 (2000) 612-621. Phase separation in hybrid Langmuir-Blodgett films of perfluorinated and hydrogenated amphiphiles. Examination by AFM.

Kaviratna and Banerjee (A.S. Kaviratna, R. Banerjee, *Colloids and Surfaces A: Physicochem. Eng. Aspects* 345 (2009) 155–162. The effect of acids on dipalmitoyl phosphatidylcholine (DPPC) monolayers and liposomes.

Kundu and Raychaudhuri (S Kundu and AK Raychaudhuri, *J Colloid Interf Sci* 353 (2011) 316-321. Effect of water and air-water interface on the structural modification of Ni-arachidate Langmuir-Blodgett films.

Mildner and Dynarowicz-Latka (J Mildner and P Dynarowicz-Latka, *Colloids Surf B* 90 (2012) 244-247. B-Carotene does not form a true Langmuir monolayer at the air-water interface.

Maheshwari and Dhathathreyan (R. Maheshwari and A. Dhathathreyan, *Journal of Colloid and Interface Science* 275 (2004) 270–276. Influence of ammonium nitrate in phase transitions of Langmuir and Langmuir–Blodgett films at air/solution and solid/solution interfaces.

Matsumoto et al (M Matsumoto, K-I Tanaka, R Azumi, Y Kondo, N Yoshino, *Langmuir* 19 (2003) 2802-2807. Structure of phase-separated LB films of hydrogenated and perfluorinated carboxylic acids investigated by IR spectroscopy, AFM and FFM.

Matsumoto et al (M Matsumoto, K-I Tanaka, R Azumi, Y Kondo, N Yoshino, *Langmuir* 20 (2004) 8728-8734. Template-directed patterning using phase-separated LB films.

Ocko et al (Benjamin M. Ocko, Michael S. Kelley, Ani T. Nikova and Daniel K. Schwartz, *Langmuir* **2002**, *18*, 9810-9815. Structure and Phase Behavior of Mixed Monolayers of Saturated and Unsaturated Fatty Acids.

Ohki et al (Shinpei Ohki, Matthias Müller, Klaus Arnold, Hiroyuki Ohshima, *Colloids and Surfaces B: Biointerfaces* **79** (2010) 210–218. Surface potential of phosphoinositide membranes: Comparison between theory and experiment.

Park (Jin-Won Park, *Colloids and Surfaces B: Biointerfaces* **71** (2009) 128–132. Individual leaflet phase effect on nanometer-scale surface properties of phospholipid bilayers.

[Petty 1996] M.C. Petty, *Langmuir-Blodgett Films, An Introduction*, Cambridge University Press, Cambridge, 1996.

Qaqish and Paige (SE Qaqish and MF Paige, *J Colloid Interf Sci* **325** (2008) 290-293. Characterization of domain growth kinetics in a mixed perfluorocarbon-hydrocarbon Langmuir-Blodgett monolayer.

[Richardson 2000] *Functional organic and polymeric materials : molecular functionality-macroscopic reality* / edited by Tim H. Richardson, Chichester : Wiley, cop. 2000.

Rodríguez et al (Ma. Rosario Rodríguez Niño, Ana Lucero, Juan M. Rodríguez Patino, *Colloids and Surfaces A: Physicochem. Eng. Aspects* **320** (2008) 260–270. Relaxation phenomena in phospholipid monolayers at the air–water interface.

Seoane et al (R Seoane, P Dynarowicz-Latka, J Miñones Jr, I Rey, *Colloid Polym Sci* **279** (2001) 562-570. Mixed Langmuir monolayers of cholesterol and essential fatty acids).

Snow et al (Arthur W. Snow, Glenn G. Jernigan, Mario G. Ancona, [Thin Solid Films](#) **556** (2014) 475–484. Equilibrium spreading pressure and Langmuir–Blodgett film formation of omega-substituted palmitic acids.

Stefaniu and Brezesinski (Cristina Stefaniu and Gerald Brezesinski, *Advances in Colloid and Interface Science* **207** (2014) 265-279. Grazing incidence X-ray diffraction



studies of condensed double-chain phospholipid monolayers formed at the soft air/water interface.

[Ulman 1990] A. Ulman, *An Introduction to Ultrathin Organic Films*, Academic Press, Boston, 1990.

Watanabe et al (S Watanabe, R Okuda, R Azumi, H Sakai, M Abe, *J Colloid Interf Sci* 363 (2011) 379-385. Effect of subphase temperature on the phase-separated structures of mixed Langmuir and Langmuir-Blodgett films of fatty acids and hybrid carboxylic acids.

Weiss et al (Martin Weis, Wei Ou-Yang, Takahiro Aida, Tetsuya Yamamoto, Takaaki Manaka, Mitsumasa Iwamoto, *Thin Solid Films* 517 (2008) 1317–1320. Study of electrostatic energy contribution on monolayer domains size.

Wydro (Paweł Wydro, [Colloids and Surfaces B: Biointerfaces](#) 106 (2013a) 217– 223. The influence of cardiolipin on phosphatidylglycerol/phosphatidylethanolamine monolayers—Studies on ternary films imitating bacterial membranes.

Wydro (Paweł Wydro, [Colloids and Surfaces B: Biointerfaces](#) 103 (2013b) 67– 74. The influence of cholesterol on multicomponent Langmuir monolayers imitating outer and inner leaflet of human erythrocyte membrane.

Wydro and Witkowska (Paweł Wydro, Karolina Witkowska, *Colloids and Surfaces B: Biointerfaces* 72 (2009) 32–39. The interactions between phosphatidylglycerol and phosphatidylethanolamines in model bacterial membranes. The effect of the acyl chain length and saturation.

Yang et al (G Yang, X Jiang, S Dai, G Cheng, X Zhang, Z Du, *Thin Solid Films* 518 (2010) 7086-7092. Morphology, defect evolutions and nano-mechanical anisotropy of behenic acid monolayer.

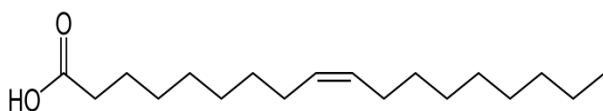
## FULL REPORT

## MATERIALS AND METHODS

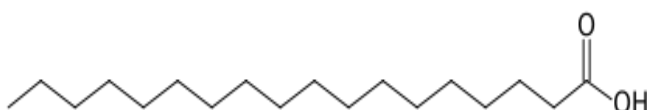
### Materials

Stearic acid (SA) was provided by Sigma-Aldrich and oleic acid (OA) by Fluka. Dipalmitoylphosphatidylcholine (DPPC) and dioleoylphosphatidylcholine (POPC) were purchased from Avanti Polar Lipids.  $\text{KH}_2\text{PO}_4$ , NaCl and chloroform of analytical grade from Sigma-Aldrich were used in solution preparation. Water was ultrapure MilliQ® (18.2  $\text{M}\Omega\cdot\text{cm}$ ).

Oleic acid is an unsaturated fatty acid with interesting properties as an agent that reduces the risk of cardiovascular illness. It is present basically in vegetable oils.

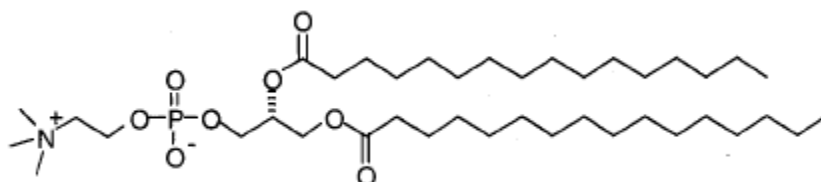


Stearic acid is the saturated form of oleic acid, and is present in vegetable and animal fats.

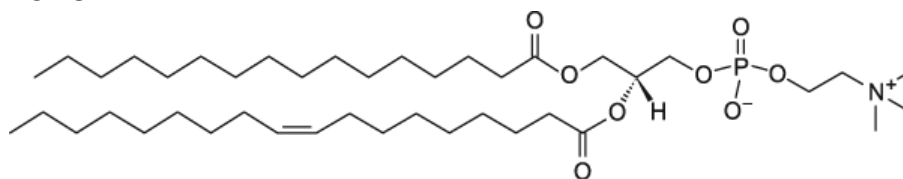


Few studies have been done concerning the mixed monolayers of these two fatty acids.

### DPPC



POPC



## Techniques

### Monolayer formation

Langmuir and Langmuir-Blodgett monolayer formation were carried on a trough (Nima Technology, Cambridge, UK) model 1232D1D2 equipped with two movable barriers. The surface pressure was measured using paper Whatman 1 held by a Wilhelmy balance connected to a microelectronic system registering the surface pressure ( $\pi$ ). The subphase used in these experiments was MilliQ® quality water. Previous to the subphase addition, the trough was cleaned twice with chloroform and once with MilliQ® quality water. Residual impurities were cleaned from the air|liquid interface by surface suctioning. The good baseline in the  $\pi$ -A isotherms confirms the interface cleanliness. Solutions of the lipids were prepared using chloroform and spread at the air|liquid interface using a high precision Hamilton microsyringe. Barrier closing rates were fixed at  $50 \text{ cm}^2 \cdot \text{min}^{-1}$  for isotherm registration and at  $25 \text{ cm}^2 \cdot \text{min}^{-1}$  for LB film transfer. No noticeable influence of these compression rates was observed on the isotherm shape. Isotherm recording was carried out adding the solution to the subphase and waiting 15 minutes for perfect spreading and solvent evaporation. Experiments were conducted at  $22 \pm 1^\circ\text{C}$  and repeated a minimum of three times for reproducibility control.

### AFM characterization

LB monolayers were transferred to mica surface for AFM characterization at defined surface pressure values. Mica surface has low roughness at a nanometric scale, which permits the best observation of the monolayer films. Mica sheets were purchased from TED PELLA Inc (CA). LB film transfer was conducted dipping the substrate, freshly cleaved mica, through the air|liquid interface on the subphase before adding the solution, and five minutes were lagged after pressure setpoint was achieved. Transfer speed was set at  $5 \text{ mm} \cdot \text{min}^{-1}$  linear velocity. The transfer ratios obtained for mica are close to 100% at each surface pressure.

The AFM topographic images of LB films were acquired in air tapping mode using a Multimode AFM controlled by Nanoscope IV electronics (Veeco, Santa Barbara, CA) under ambient conditions. Triangular AFM probes with silicon nitride cantilevers and silicon tips were used (SNL-10, Bruker) which have a nominal spring constant  $\approx 0.35 \text{ N}\cdot\text{m}^{-1}$  and a resonant frequency of 50 kHz. Images were acquired at 1.5 Hz line frequency and at minimum vertical force to reduce sample damage. AFM images were obtained by scanning several macroscopically separated areas on each sample.

## RESULTS

### 1. Oleic acid, stearic acid and their mixtures

#### 1.1 Oleic acid (OA) [Ácido Oleico (AOL)]

##### Isotherms

Surface pressure-area isotherms of OA monolayers have been done in several conditions. It is observed a null o small influence of the compression speed. Three subphases have been used: water, saline solution and saline-phosphate solution. It is observed a small influence of the subphase, especially at high surface pressures. The collapse pressure depends on the subphase, and a higher collapse pressure is observed in the presence of phosphate.

Calculating the elastic modulus  $C_s^{-1}$  (inverse of the compressibility coefficient), a LE state is obtained for the OA monolayer. The monolayer becomes a little more fluid in presence of phosphate. The maximum values found for  $C_s^{-1}$  are: around 85 m/mN in water, around 85 in NaCl solution, and around 65 for NaCl+phosphate solution.

An analysis of the isotherms using the virial state equation has been done.

The plot of  $PA/(kT)$  vs  $P$  can be adjusted with a polynomial de  $2n$  degree,  $PA/(kT)=b_0+b_1P+b_2P^2$ , where  $b_0$ ,  $b_1$  and  $b_2$  are the virial coefficients.

obtaining for the water subfase the parameters  $b_0=0.0055$ ,  $b_1=0.1255$ ,  $b_2=-0.0015$ .

Obtaining for the nacl subphase  $b_0=0.0068$ ,  $b_1=0.1292$ ,  $b_2=-0.0015$ .

Obtaining for the nacl+phosphate subphase  $b_0=0.0226$ ,  $b_1=0.133$ ,  $b_2=-0,0018$ .

AFM images (not shown) present a uniform morphology at several surface pressures due to the LE state.

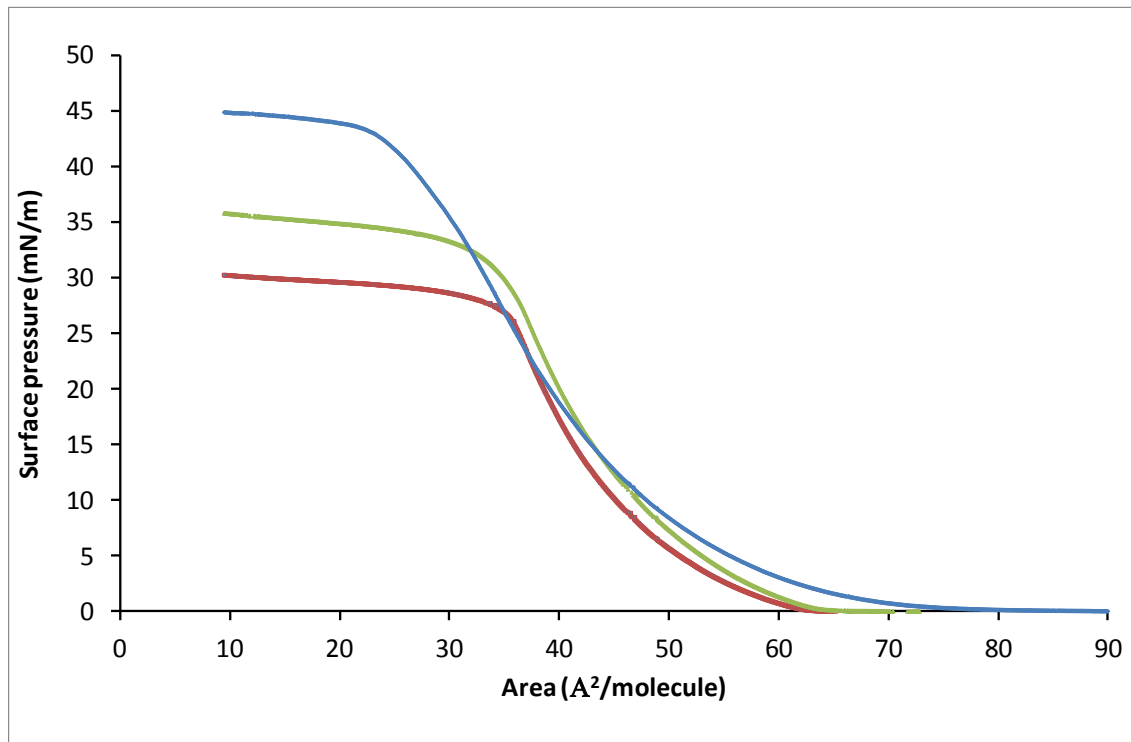


Figure 1. Isotherms of oleic acid (AOL) on different subphases. Temperature of 21-22°C (21.5°C). 1 water (brown, 4 NaCl (green, and 7 NaCl+phosphate (blue.

$C(\text{AOL})=0.54 \text{ mg/mL}$ .  $V=50 \text{ cm}^2/\text{min}=4.3 \text{ Å}^2/\text{molec min}$

\*

Aigua:1-3  $v=50 \text{ cm}^2/\text{min}=4.3 \text{ Å}^2/\text{molec min}$

NaCl:4-6  $v=50$

+fosfat: 7-9  $v=50$  la 7 no te baixada, 10-12 no tenen baixada alguns altres si (encara que la  $v=25$ )

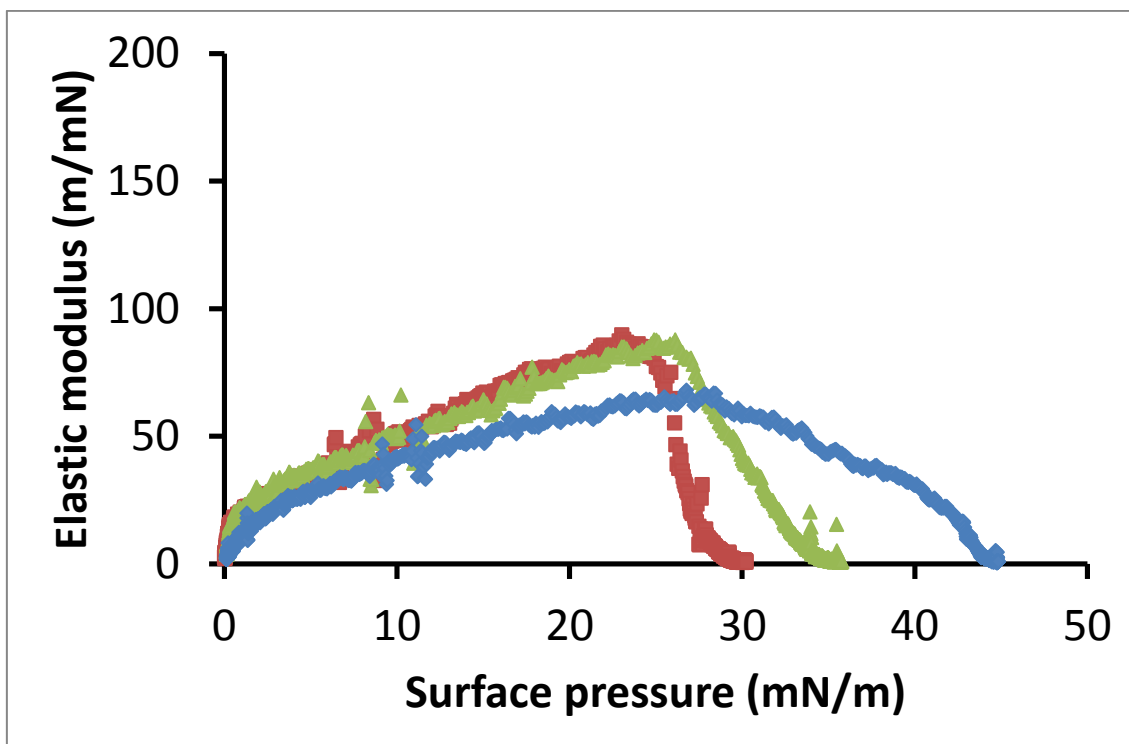
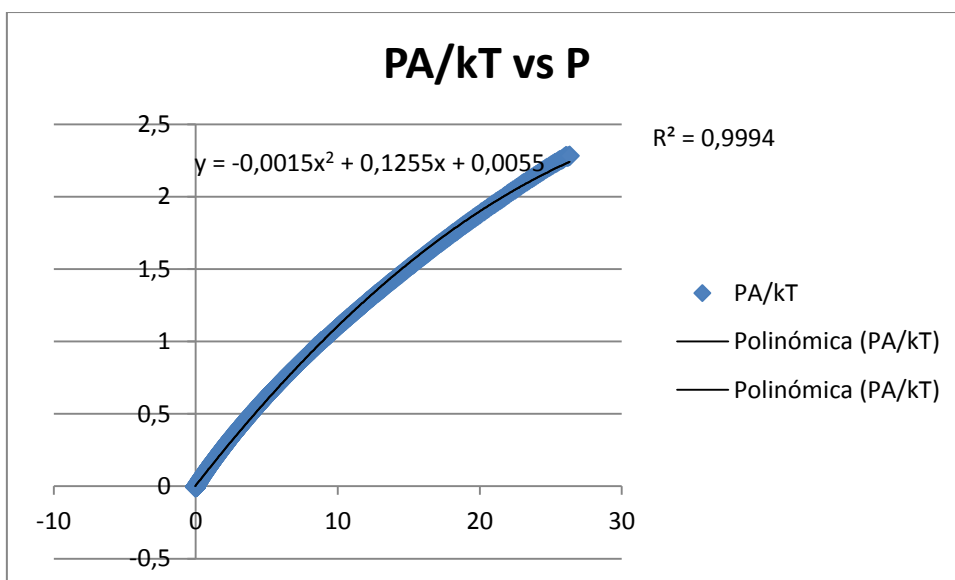
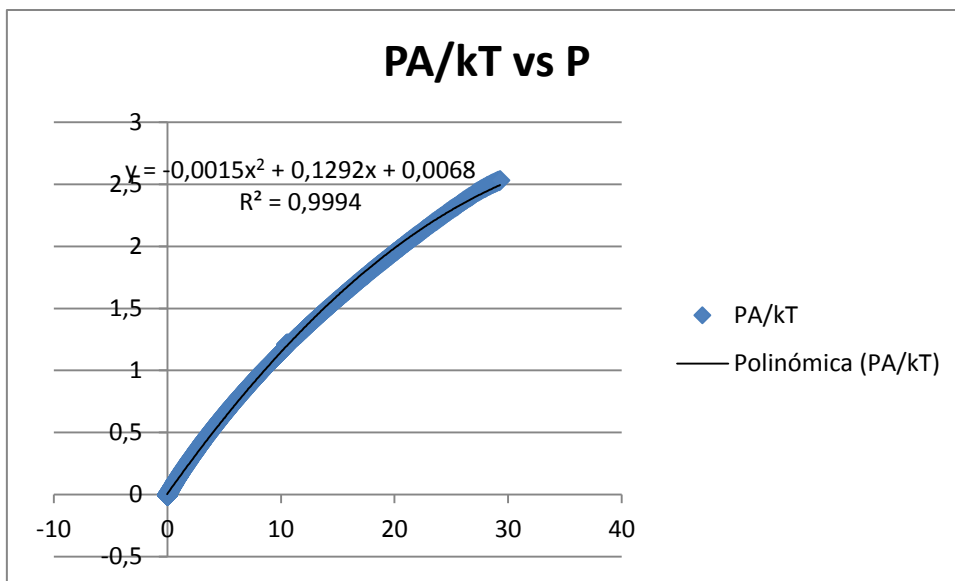


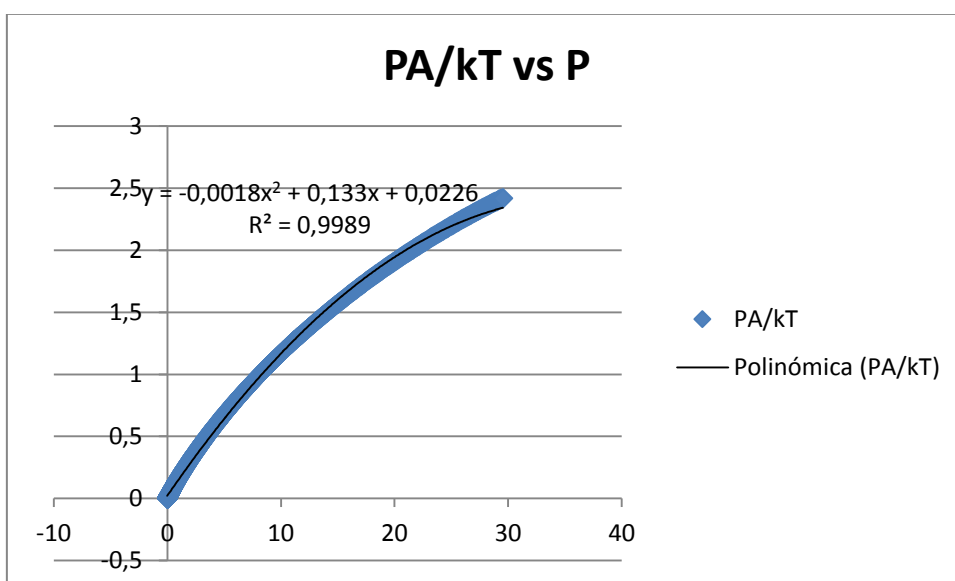
Fig 2. Elastic modulus  $C_s^{-1}$  for oleic acid. Colours as in Fig 1. 1 marro, 4 verd, 7 blau.



OA in water subphase



In NaCl



In NaCl+fosfat subphase

Fig 3. State equation plots for oleic acid.

## Discussion

The values of  $b_1$  increase slightly when NaCl and NaCl+ phosphate are present in the subphase. As these values of  $b_1$  are positive, indicate an increase of the repulsive interactions. On the other hand, the values of  $b_0$  are also higher in presence of NaCl and especially of NaCl+phosphate. Higher values of  $b_0$  indicate less aggregation. These results are coherent with a more fluidity of the film in the presence of these salts, especially of NaCl+phosphate (Fig C<sub>s</sub><sup>-1</sup>).

When comparing isotherms of oleic acid and oleamide (Torrent 2011) some slight differences can be observed in the isotherm going up, but especially in the collapse pressure.



## 1.2 Stearic acid (SA). [Ácido esteárico (AE)].

Surface pressure-area isotherms for SA have been recorded in several subphases: water, saline solution and saline-phosphate solution. There is a small influence in the isotherms, especially at high surface pressures, presenting the saline and saline-phosphate subphases a higher collapse pressure.

Collapse pressure on water subphase= 57 mN/m

Collapse pressure on saline subphase=62

Collapse pressure on saline-phosphate subphase=62

The isotherm of SA presents several inflexion points where the slope change, which could correspond to phase changes in the monolayer. These points are better seen in the elastic modulus plot. These points are located at around  $P=10$  mN/m,  $P=22-24$  mN/m and  $42$  mN/m. According to the values of the elastic modulus, LC states can be present at  $P<22-24$ , with a change from a LC1 to a LC2 at around  $P=10$  mN/m where an inflexion appears. This change do not produces a significant change in the elastic modulus, and is practically the same in the three subphases. At  $P>24$  mN/m a S state is obtained, that can present a tilting change at around  $42$  mN/m for the NaCl and NaCl+phosphate subphases. In this case, this change produces a significant increment in the elastic modulus (Fig  $C_s^{-1}$ ), but does not reach the value for the water subphase.

State equation

An analysis of the isotherms using the virial state equation has been done.

The plot of  $PA/(kT)$  vs  $P$  can be adjusted with a polynomial de  $2n$  degree,  $PA/(kT)=b_0+b_1P+b_2P^2$ , where  $b_0$ ,  $b_1$  and  $b_2$  are the virial coefficients.

obtaining for the water subfase the parameters  $b_0=-0.0021$ ,  $b_1=0.0566$ ,  $b_2=-0.00018$ .

Obtaining for the nacl subphase  $b_0=-0.0024$ ,  $b_1=0.0598$ ,  $b_2=-0.00023$ .

Obtaining for the nacl+phosphate subphase  $b_0=0.0025$ ,  $b_1=0.0589$ ,  $b_2=-0,00021$ .

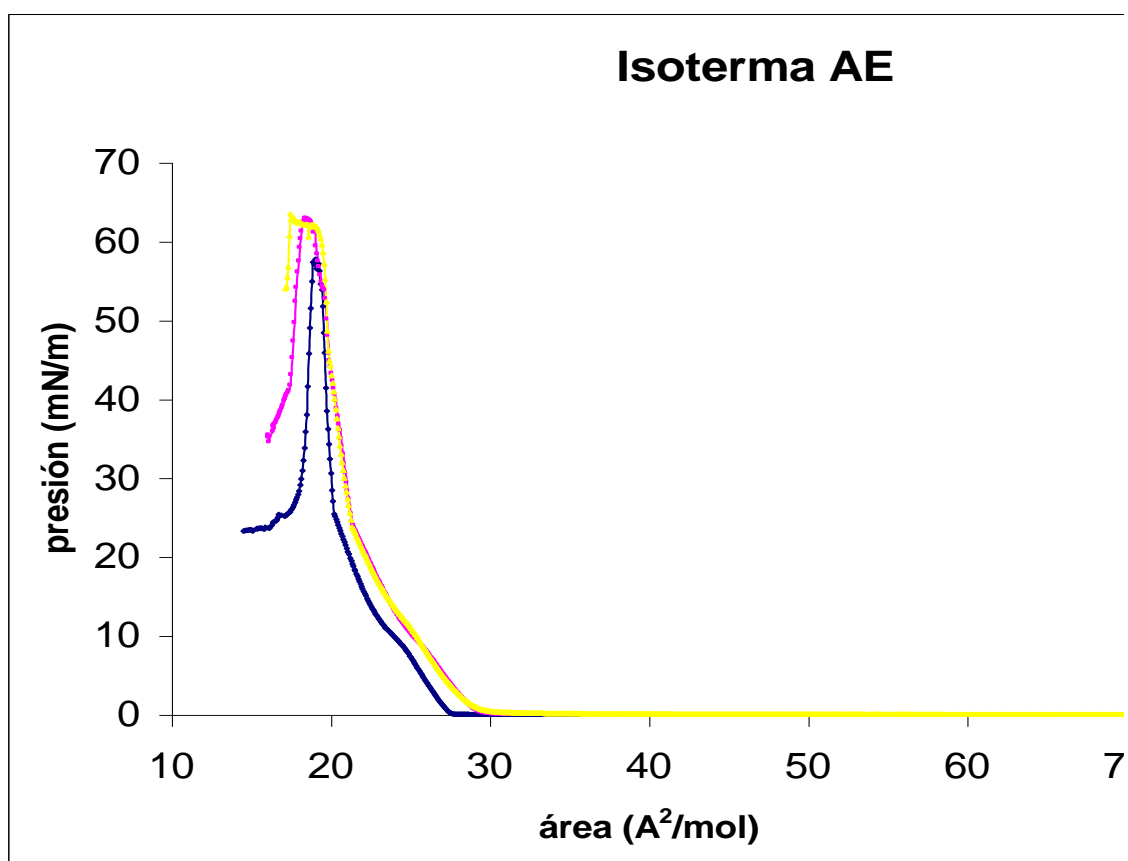
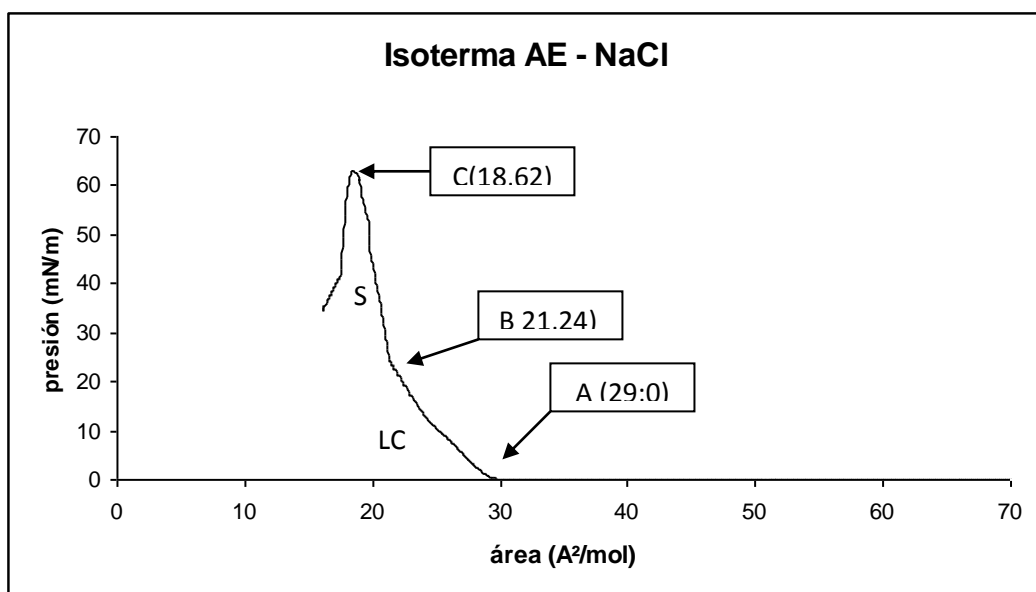
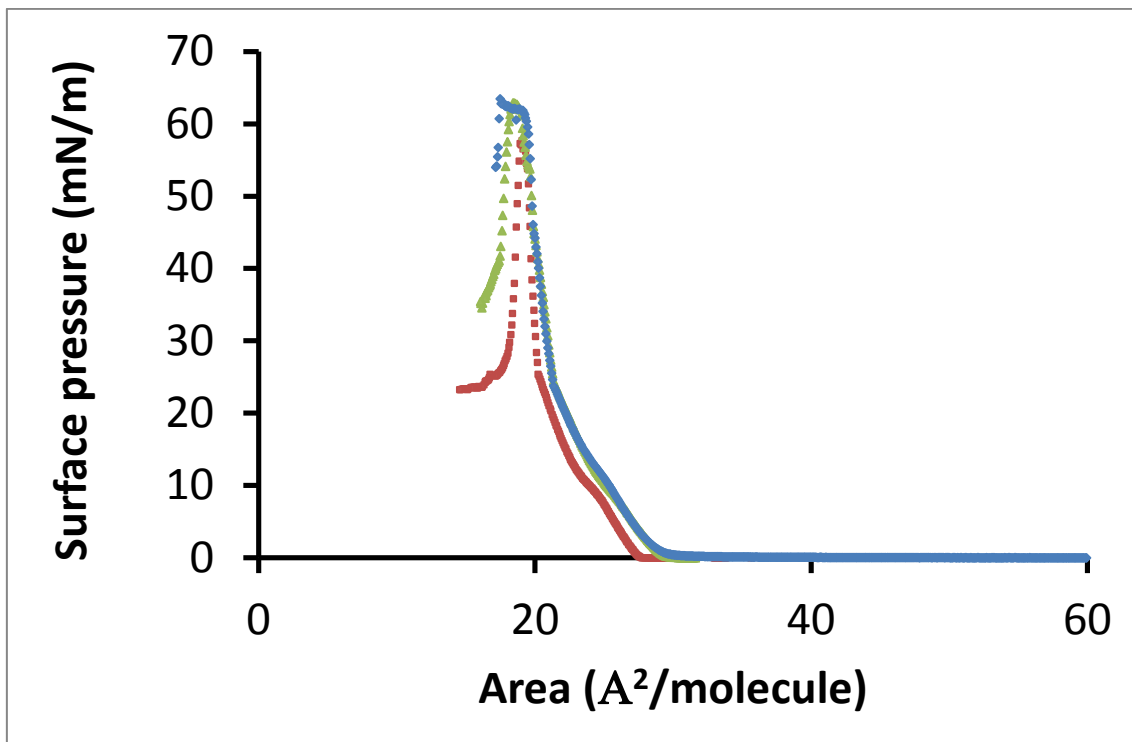


Figura 4. Isotherms of stearic acid (AE) in different subphases: blue) water, magenta) NaCl, yellow) NaCl+phosphate. (Temperature 21-22°C).



Isotherms for SA: brown water 4, green NaCl 5, blue NaCl+fوسفات 10

$C(\text{SA}) = 0.49 \text{ mg/mL}$ .  $V = 50 \text{ cm}^2/\text{min} = 4.8 \text{ Å}^2/\text{molec min}$

Figura 4. Isotherms of stearic acid (AE) in different subphases. Temperature of 21-22°C (21.5°C)

\*

Aigua: 1-4

Nacl:5-7

Fوسفات:8-10

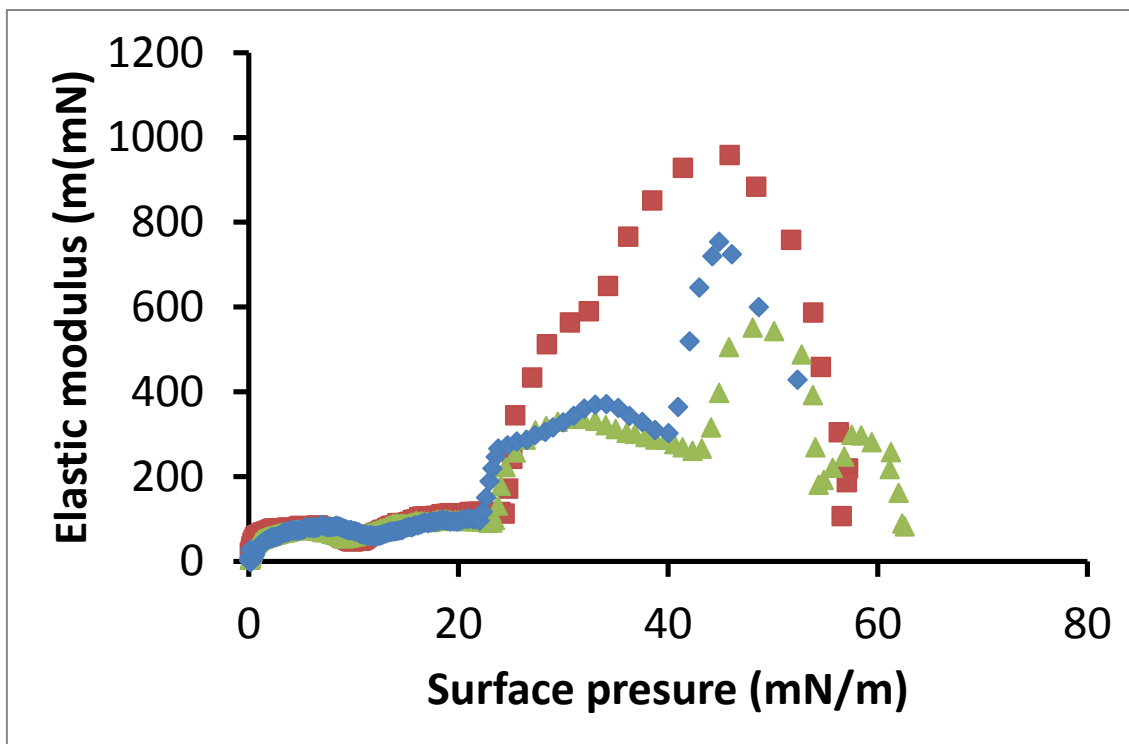
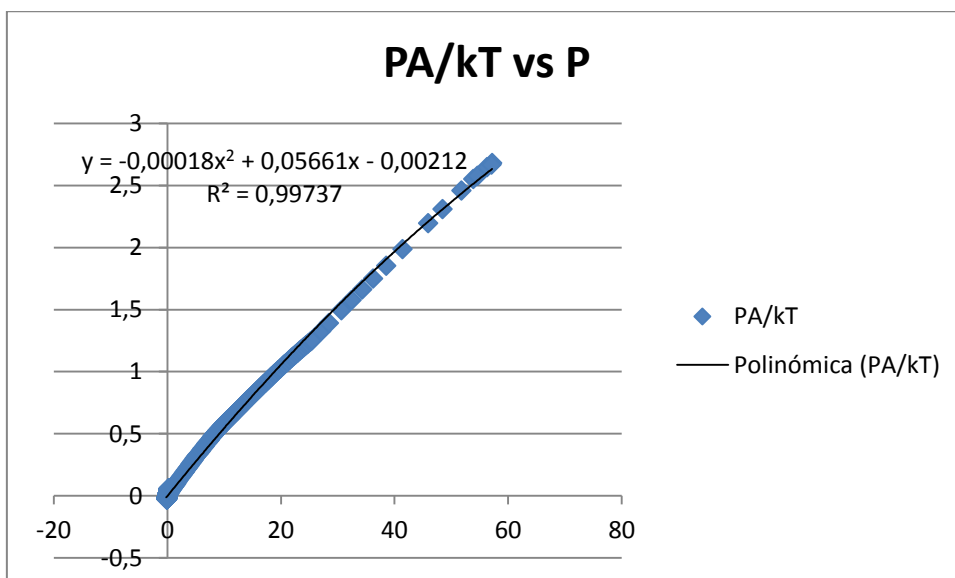
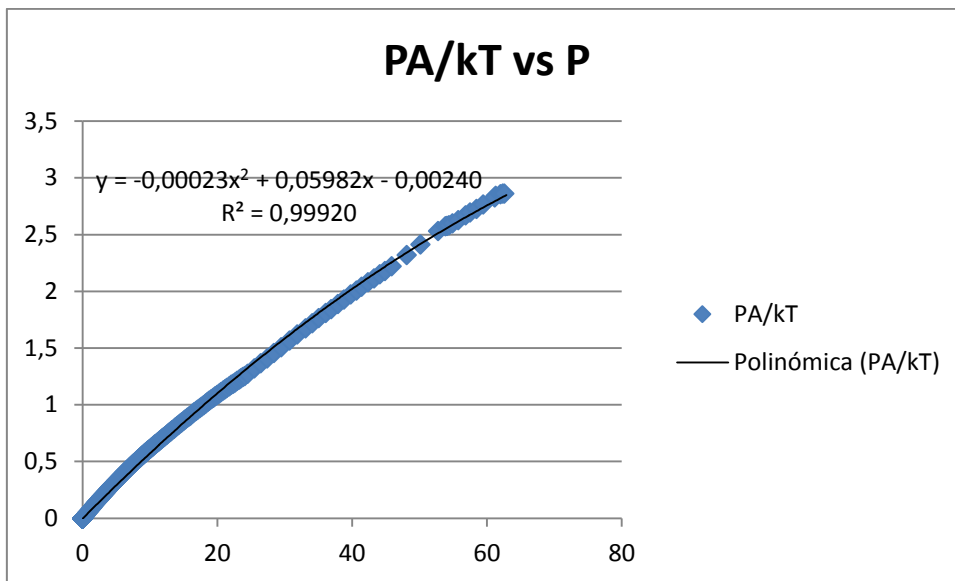


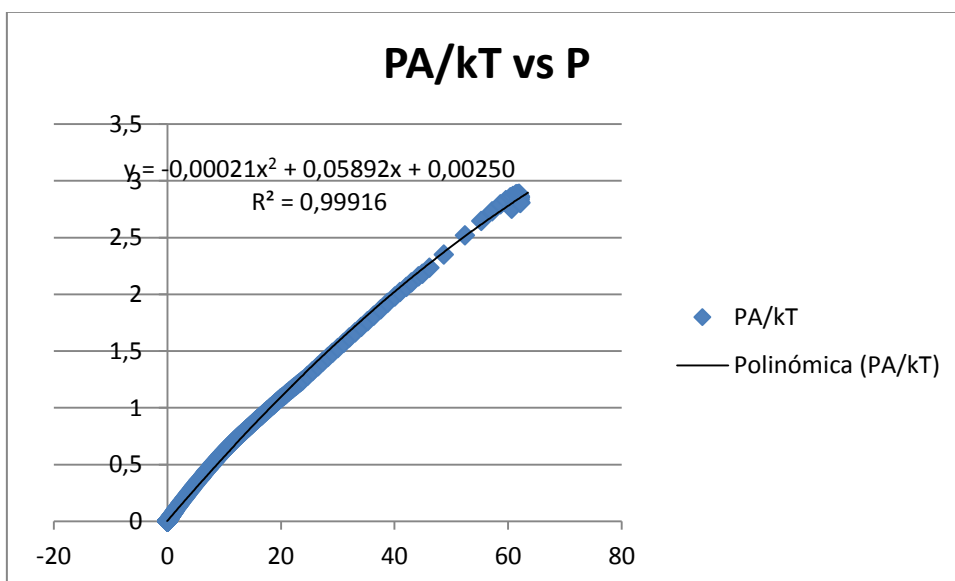
Fig 5. Elastic modulus  $C_s^{-1}$ : Colours as in Fig 4. 4 marro, 5 verd, 10 blau.



In water



In NaCl



In NaCl+fosfat

Fig 6. Sate equation plots for SA.

## Discussion

The presence of NaCl and NaCl+phosphate produces a slightly decrease in the values of  $C_s^{-1}$  at the most compact state, indicating that these salts difficult the rigid compactness of the monolayer.

The values of  $b_1$  increases slightly when NaCl and NaCl+ phosphate are present in the subphase. As these values of  $b_1$  are positive, indicate an increase of the repulsive interactions. On the other hand, the values of  $b_0$  are also slightly higher in presence of NaCl+phosphate. Higher values of  $b_0$  indicate less aggregation. These results are coherent with a less rigidity of the film in the presence of these salts (Fig  $C_s^{-1}$ ). Nevertheless the values of  $b_0$  are close to 0 indicating a high degree of aggregation.

As the values of  $b_1$  for SA are lower than those of OA, this fact indicates higher repulsive interactions between OA molecules in respect to SA ones. On the other hand, the values of  $b_0$  for SA are lower than those of OA, this fact indicates higher aggregation between SA molecules in respect to OA ones.

## 1.2 STEARIC ACID (II)

### Anàlisi de la isoterma:

La velocitat de la FER es de 10, 20 cm<sup>2</sup>/min, i potser es podria veure si hi ha influència de la velocitat (a igual temperatura). Potser si, a velo baixa la iso puja a arees menors.

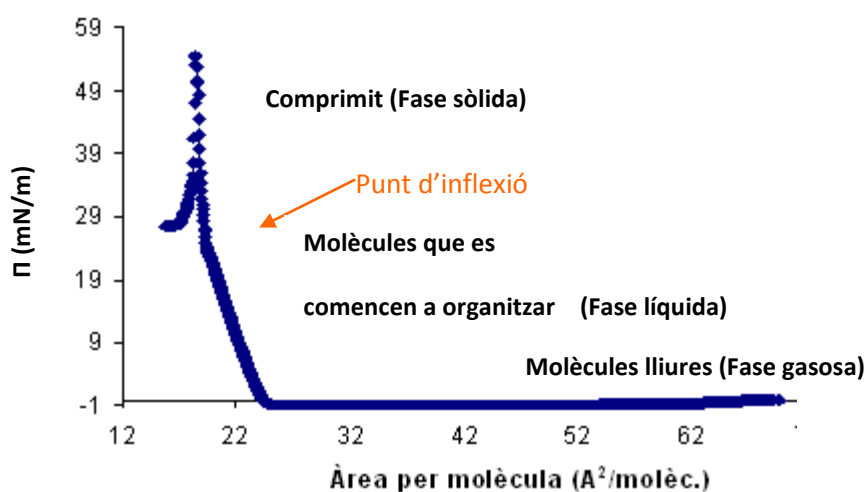


**Figura 1.2.3.** Representació d'una isoterma Langmuir d'àcid esteàric a 21°C.

Tal i com es mostra, l'SA presenta la típica isoterma Langmuir amb un punt d'inflexió a una  $\Pi$  de 24 mN/m.

### Comparació a dues temperatures diferents:

Duent a terme el procediment experimental es va observar que, representant les dades, apareixia un desplaçament d'àrea per molècula a valors més grans quan la temperatura de treball era uns graus més alta que la de costum, 21°C. Això és degut a què només uns quants graus de diferència afecten molt a la isoterma, tal i com es veu teòricament.

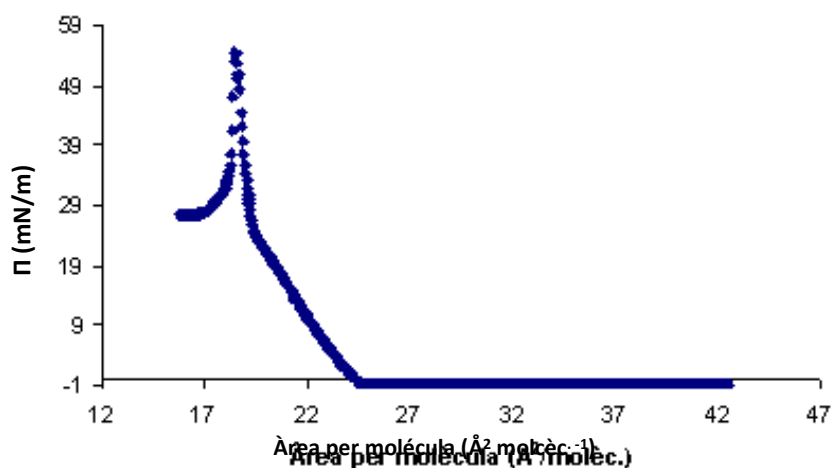


**Figura 1.2.4.** Representació d'una isoterma Langmuir d'àcid esteàric a 21°C.

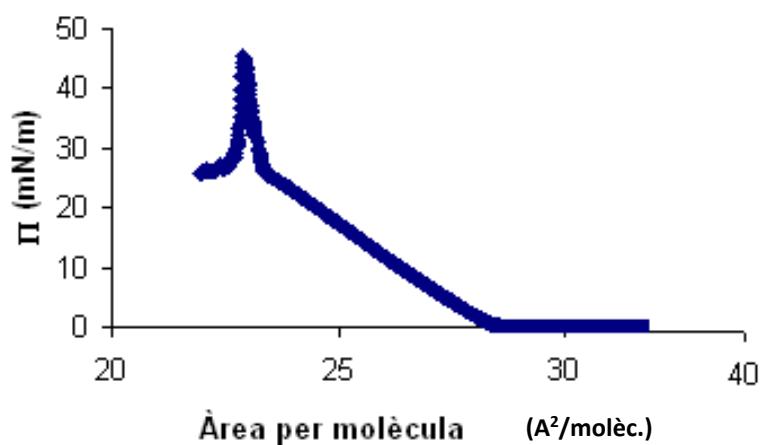


**Figura 1.2.5.** Representació d'una isoterma Langmuir d'àcid esteàric a 28°C.

Aquest efecte és degut a què quan la temperatura augmenta hi ha més agitació tèrmica i la pressió superficial creix abans. A més a més, també s'arriba a abans al col·lapse degut a què no té prou temps per a comprimir-se correctament.

Effect of temperatura:

Increasing temperatura: the collapse pressure decreases, the inflexion point (change from LC to S) increases, the lift-off area increases.



### Càlcul del factor de compressibilitat:

A través de l'estudi Langmuir s'ha calculat el factor de compressibilitat de l'SA amb l'equació.

$$\beta = \frac{-1}{A} \left( \frac{\partial A}{\partial \pi} \right)_T$$

On  $\beta$  és la constant de compressibilitat ( $\text{m mN}^{-1}$ ),  $A$  l'àrea per molècula ( $\text{\AA}^2 \text{mol}^{-1}$ ) i  $\Pi$  la pressió superficial ( $\text{mN m}^{-1}$ ).

dues isoterms Langmuir, una a una temperatura de  $24^\circ\text{C}$  i l'altre a  $28^\circ\text{C}$  (figura 1.2.6A i B) i es calcula beta.

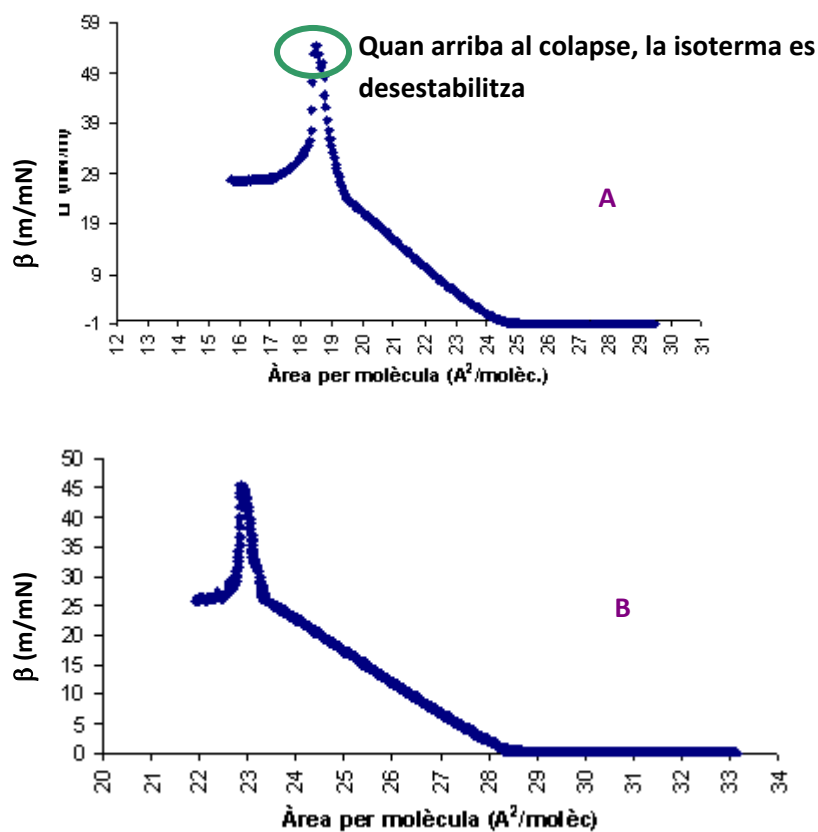


**Figura 1.2.6.** Representació d'una isoterma Langmuir d'àcid esteàric a A)  $24^\circ\text{C}$  i B)  $28^\circ\text{C}$ .

D'aquesta manera es poden obtenir les representacions gràfiques del factor de compressibilitat en front la  $\Pi$  ( $\text{mN/m}$ ) tal i com es mostra en les figures 1.2.7.

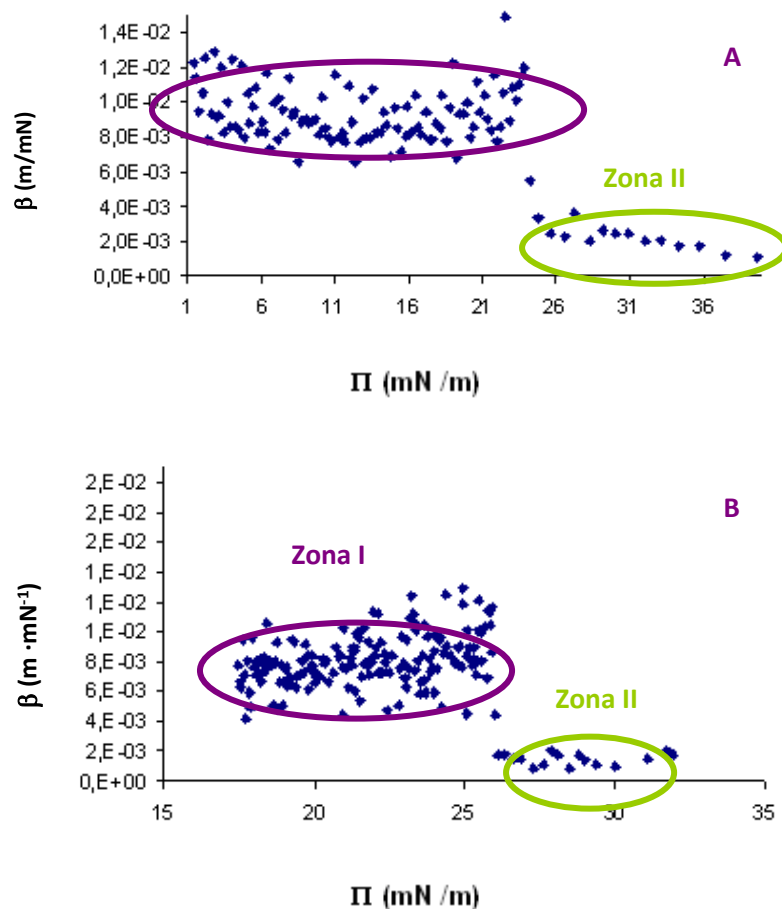


**Figura 1.2.7.** Representació del factor de compressibilitat en funció de la  $\Pi$  a

A) 24°C i B) 28°C.

Stearic acid presents two physical states. Below the inflexion point (around 24 mN/m depending on temperature) it presents a LC state, meanwhile above this inflexion point it presents a S state.

The inflexion point depends on temperature: it is around 24mN/m at 21°C, it is 24 mN/m at 24°C and 26 mN/m at 28°C.

El valor del factor de compressibilitat quan la temperatura és de 24°C és de  $8'3 \cdot 10^{-3}$  m/mN en la primera zona (FASE LC), força similar al trobat bibliogràficament [1] [2] i en la segona zona de  $1'1 \cdot 10^{-3}$  m/mN (fase S).

Per a una temperatura de 28°C en la primera zona s'obté un valor de  $8'8 \cdot 10^{-3}$  m/mN (fase LC) i un valor  $1'0 \cdot 10^{-3}$  m/mN en la segona zona (fase S).

At low temperatures, as 21°C, the isotherm also presents a weak inflexion at around 10 mN/m, but the physical state does not change (LC). This probably indicates a tilting change, a change from a LC1 state to a LC2 state.

[1] Petty, Michael C., Langmuir – Blodgett Films, an Introduction

Cambridge University Press, 1996

[2] Sergi Garcia-Manyés et al. Volume 1768, Issue 5, May 2007, Pages 1190-1198

### **Estudi topogràfic per AFM:**

Since SA presents condensed states and phase changes, AFM images can be done showing them.

Es van extreure vàries monocapes d'àcid esteàric a temperatura ambient (24°C) a diferents pressions, com són: 1, 5, 10, 15, 20, and 25 and 35 !! mN·m<sup>-1</sup>.

Es pot observar que la pressió no es manté a 35 mN/m sinó que disminueix a aproximadament a un valor de 25 mN m<sup>-1</sup>. Com s'hauria de mantenir la pressió sense problemes a un valor de 35 mN m<sup>-1</sup>, ja que pot arribar a valors superiors tal i com es veu en la figura 23, es va repetir el procediment vàries vegades obtenint-se el mateix resultat. Creiem que la fase és inestable, es col·lapse i retorna al valor del punt d'inflexió.

De totes les extraccions es van obtenir imatges topogràfiques tal i com es mostra en la seqüència següent (figura 1.2.8 i 1.2.9).

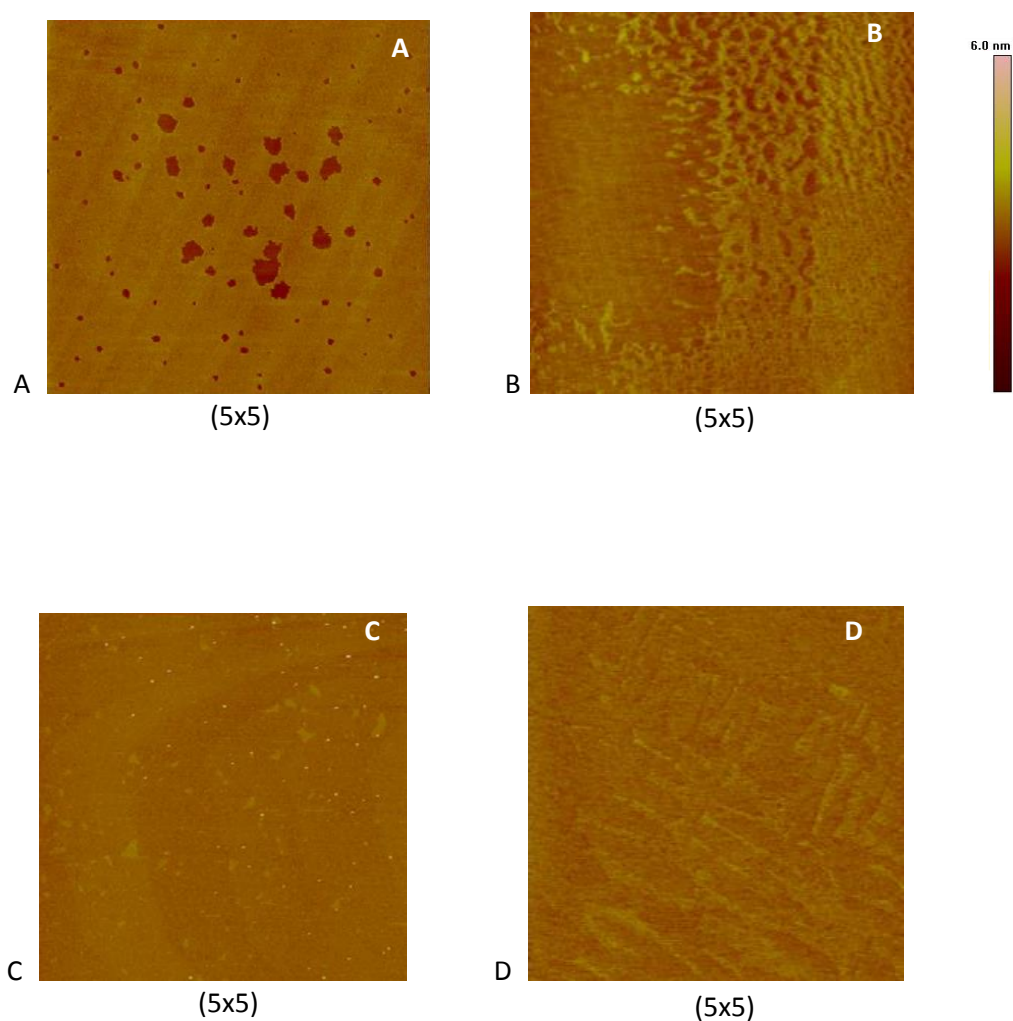


**Figura 1.2.8.** TAPPING MODE A)  $\Pi = 1 \text{ mN m}^{-1}$ , B)  $\Pi = 10 \text{ mN m}^{-1}$ , C)  $\Pi = 15 \text{ mN m}^{-1}$ , D)  $\Pi = 20 \text{ mN m}^{-1}$

La figura 1.2.8A mostra una sola fase. La  $\Pi$  ( $1 \text{ mN m}^{-1}$ ) és tant baixa que ni tant sols es pot arribar a formar una monocapa completa deixant forats en tota la seva superfície. En la 1.2.8B ja es veuen dues fases, la primera fase es disposa a sota i cobreix completament la mica mentre que es comença a veure una segona fase, es coneix perquè presenten diferents alçades. Es va veient la evolució amb les figures 1.2.8C i 1.2.8D on, al anar augmentat la  $\Pi$ , s'observen diferents orientacions de la molècula.

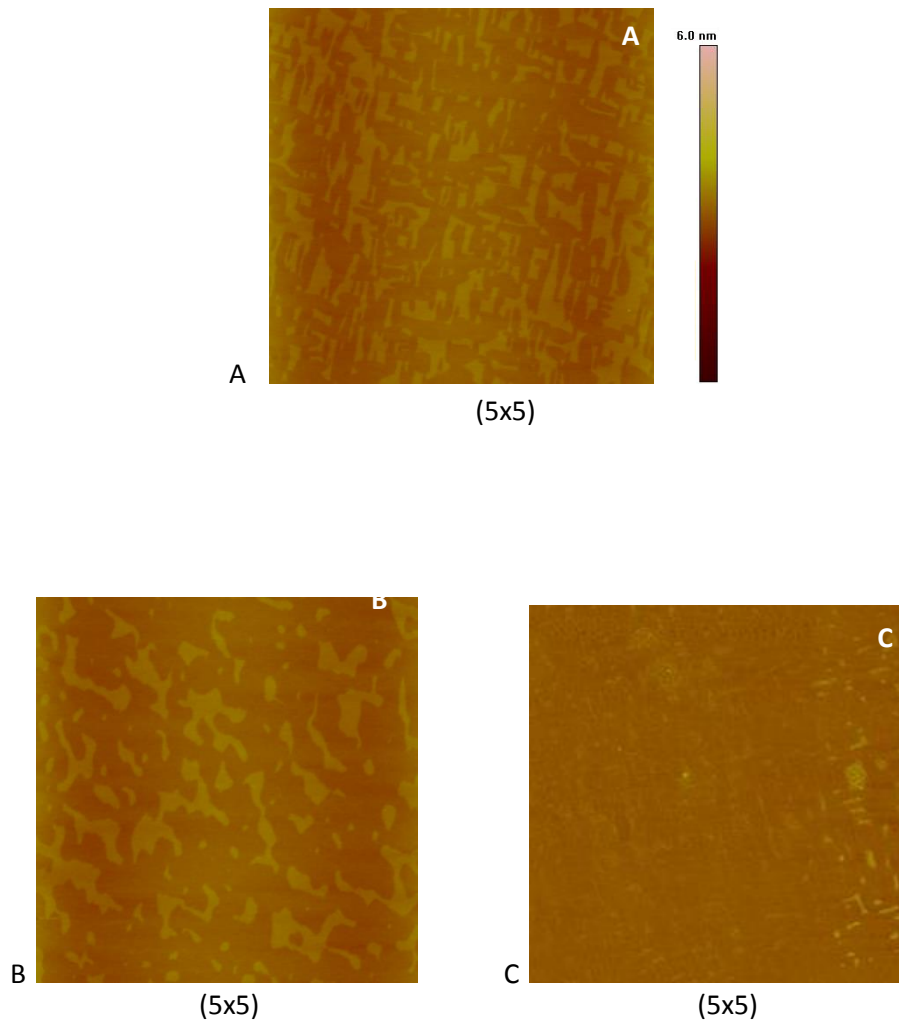


**Figura 1.2.9.** tapping mode A)  $\Pi = 25 \text{ mN m}^{-1}$  B)  $\Pi = 25 \text{ mN m}^{-1}$  C)  $\Pi = 35 \text{ mN m}^{-1}$

En la 1.2.9A i 1.2.9B també es veuen dues fases ja que mostren diferents alçades però es presenten en ordenacions diferents en una i altra, segurament degut a diferents graus d'inclinació que la molècula ha anat adoptant a mesura que s'ha anat augmentant la  $\Pi$ . Finalment, la 1.2.9C mostra una imatge on hi ha una diferència important d'alçada des de la zona més baixa i la zona més alta, creiem que degut a què les molècules han col·lapsat i s'han desordenat.

#### **Anàlisi de les seccions topogràfiques.**

Es coneix que l'alçada d'una molècula d'SA quan està completament estirada és de 2.5 nm.

Es va decidir realitzar un anàlisi d'alçades de les imatges presentades en les figures 1.2.8 i 1.2.9 per a poder conèixer amb més detall les fases presents en cada cas. Amb el programa informàtic Nanoscope 5.12 es van analitzar les seves seccions a partir de la profunditat.

L'estudi de l'alçada existent entre els dos nivells que s'observen en les imatges de topografia obtingudes per mitjà de l'anàlisi de la secció transversal dona els valors que es presenten en la taula.

**Taula.** Valors obtinguts de les imatges de seccions.

<b>Figura</b>	<b>Alçada per contacte intermitent (nm)</b>	<b>Alçada per corbes de força (nm)</b>
34A	0.689	1.122
34B	0.275	-----
34C	0.284	1.129
34D	0.242	1.454
35A	0.226	-----
35B	0.257	-----
35C	0.160	1.751

S'observa que quan la molècula està relaxada es mostra amb una alçada d'uns 0.689 nm. Quan la pressió que s'exerceix és de 10 o 15 mN m<sup>-1</sup> apareixen dues orientacions de la molècula on la diferència entre alçades és d'aproximadament 0.280 nm. Compactant més, l'SA va canviant d'inclinació i la diferència d'alçades va variant. Curiosament es mostren alçades diferents però força similars fet que fa pensar que es pot tractar de la molècula amb dos graus d'inclinació diferents a la mateixa  $\Pi$ . Una altra figura mostra una diferència d'alçades bastant diferent de la resta degut a què la molècula s'acosta al seu col·lapse amb una diferència d'alçades de només 0.160 nm.

## Espectroscopia de Forces: Estudi del trencament de capes

Per mitjà de l'espectroscòpia de forces es va realitzar l'estudi de la propietat nanoelàstica de varies monocapes d'SA extretes a diferents  $\Pi$ . Es van obtenir aproximadament unes 270 corbes de força de diferents zones de la superfície de cada mostra.

D'aquesta manera, es pot obtenir doble informació del gràfic, per una banda, la força necessària per a trencar una monocapa i, per l'altre, el gruix d'aquesta (Figura 1.2.12).

El valor de la força necessària per a assolir el trencament de la monocapa en cada cas varia així que, en cada una de les corbes de força tractades es van representar tots els valors, a fi d'obtenir un histograma estadístic que permetés mostrar una distribució d'aquesta força. (Figura 1.2.13 A, B i C).

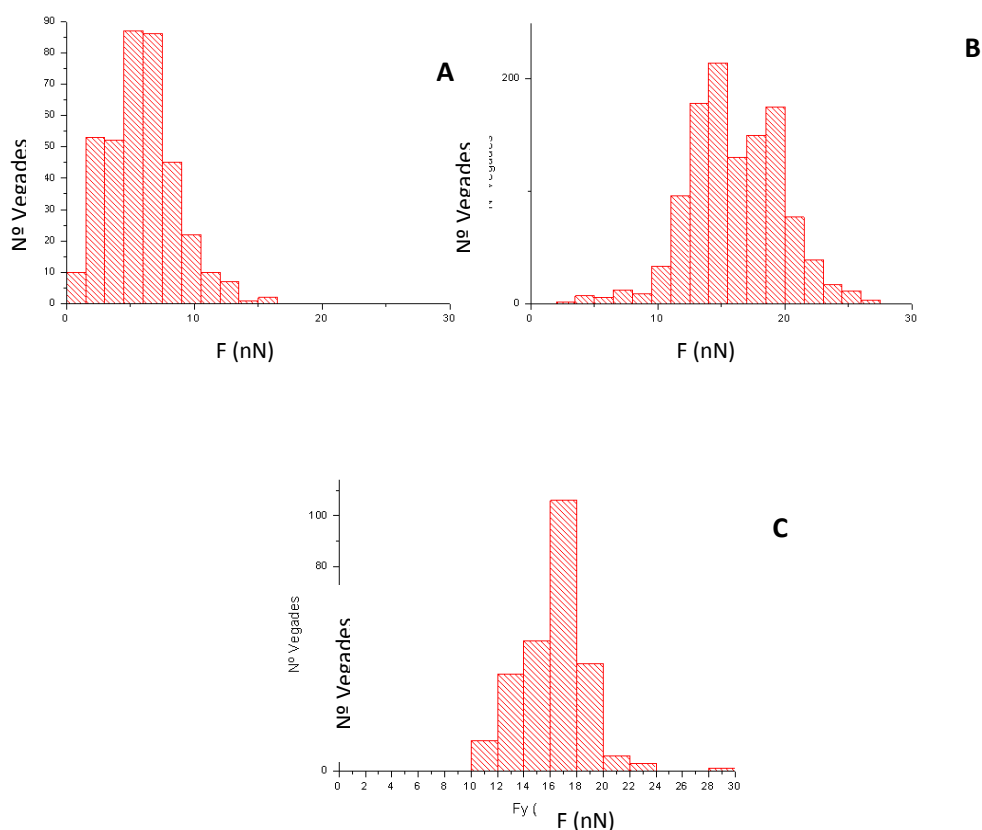


**Figura 1.2.13.** Histogrames de la distribució de la força de trencament necessària per a penetrar una monocapa d'SA. En l'eix d'ordenades s'hi representa el nombre de vegades que es repeteix un valor i en les abscisses el valor de la força emprada per trencar la monocapa (nN). A)  $1 \text{ mN m}^{-1}$  B)  $20 \text{ mN m}^{-1}$  i C)  $35 \text{ mN m}^{-1}$

Es pot observar que a mesura que la  $\Pi$  augmenta, també ho fa la força, desplaçant-se a valors cada vegada més alts. La monocapa, a mesura que augmenta la  $\Pi$ , necessita més força per a ser trencada ja que també augmenta el grau de compactació de la monocapa, fent-se més difícil la penetració de la punta per estudiar la seva FC.

For  $p=1$  mN/m the breaking force is  $7.8 \pm 2.7$  nN and for  $p=20$  mN/m it is  $16.0 \pm 3.7$  nN, as can be expected the breaking force increases with increasing the surface pressure [ref nostra AA].



### 1.3 Mixed SA and OA. [Ácido oleico y ácido esteárico (AOL+AE)]

Several mixtures of SA and OA have been prepared and their surface pressure-area isotherms have been obtained:

Temperature 21-22°C

- 80% de AOL + 20% de AE,  $X(\text{OA}) = 0.816$
- 60% de AOL + 40% de AE 0.625
- 40% de AOL + 60% de AE 0.425
- 20% de AOL + 80% de AE 0.217

Figure 7 shows these isotherms together to those of pure SA and pure OA.

Mixed monolayers shows a first collapse that practically coincides with that of OA, and when the proportion of SA increases, a second collapse is observed which does not reaches the value observed for SA. This is an indication that at high surfaces pressures, OA forms a separated phase from SA and collapse at its surface pressure.

A study of the mean area per molecule (Fig 8) shows positive deviations from the straight line, being these deviations more important at low surface pressures and when the OA content is 40%. At high surface pressures and all compositions except for the OA content of 40%, the mean area is close to the straight line. Positive deviations indicate mixing but with unfavorable interactions in respect to pure components. Null deviations indicate ideal mixing or phase separation.

Pero para esclarecer esto deben realizarse otros experimentos, como la formación de películas LB y su observación por AFM.

Elastic modulus for mixtures is plot in Fig 9 .

Mixtures show a LE state, but when the SA content is high, a LC state appears at higher surface pressures.

It is also seen that when the SA content increases, the surface pressure at the inflexion point in the isotherm, or at the maximum point in the compressibility plot, decreases.

The results point to a partial mixing at low surface pressures but a segregation at high surface pressures, especially at high SA content.

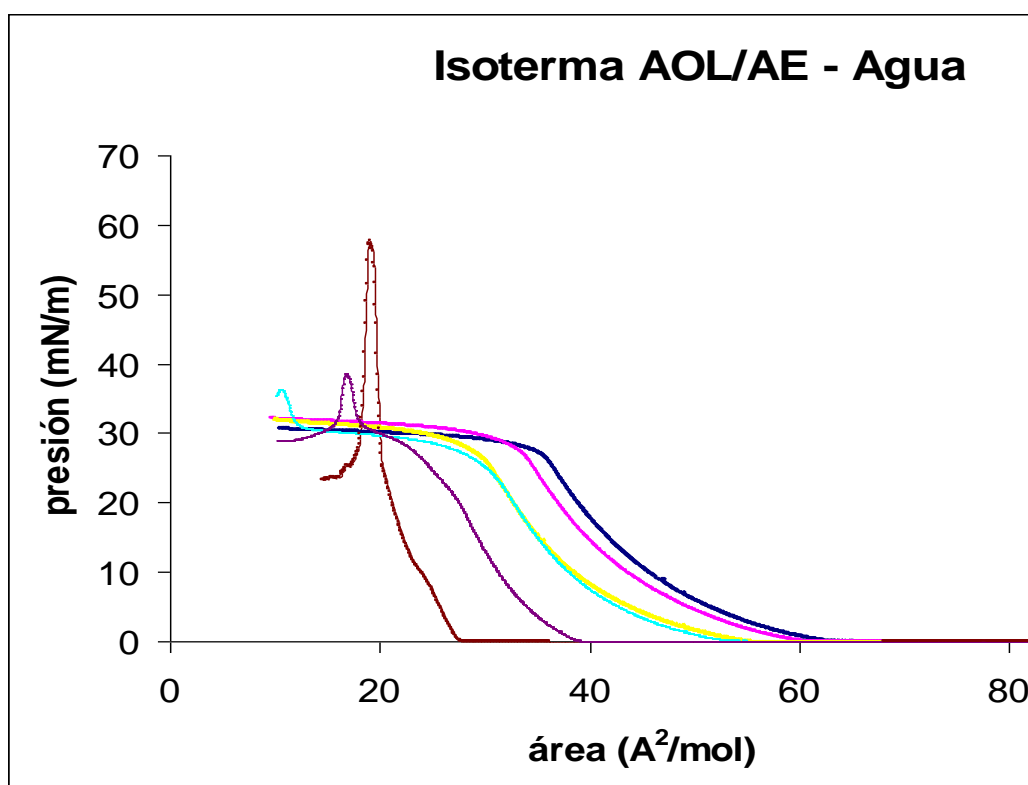


Figura 7. Isotermas de monocapas de mezclas AOL+AE. Azul) AOL, magenta) 80:20, amarillo) 60:40, cian) 40:60, violeta) 20:80, marrón) AE.

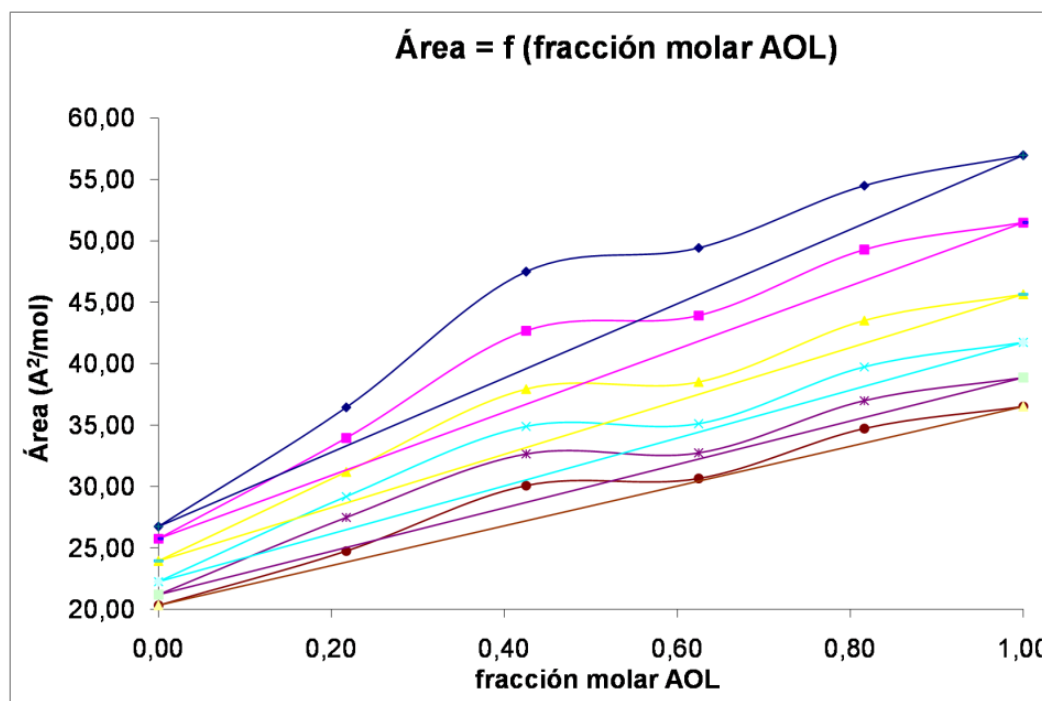


Figura 8. Area vs composición en mezclas AOL+AE, a diferentes presiones superficiales: azul) 2, magenta) 5, amarillo) 10, cian) 15, violeta) 20, marrón) 25 mN/m.

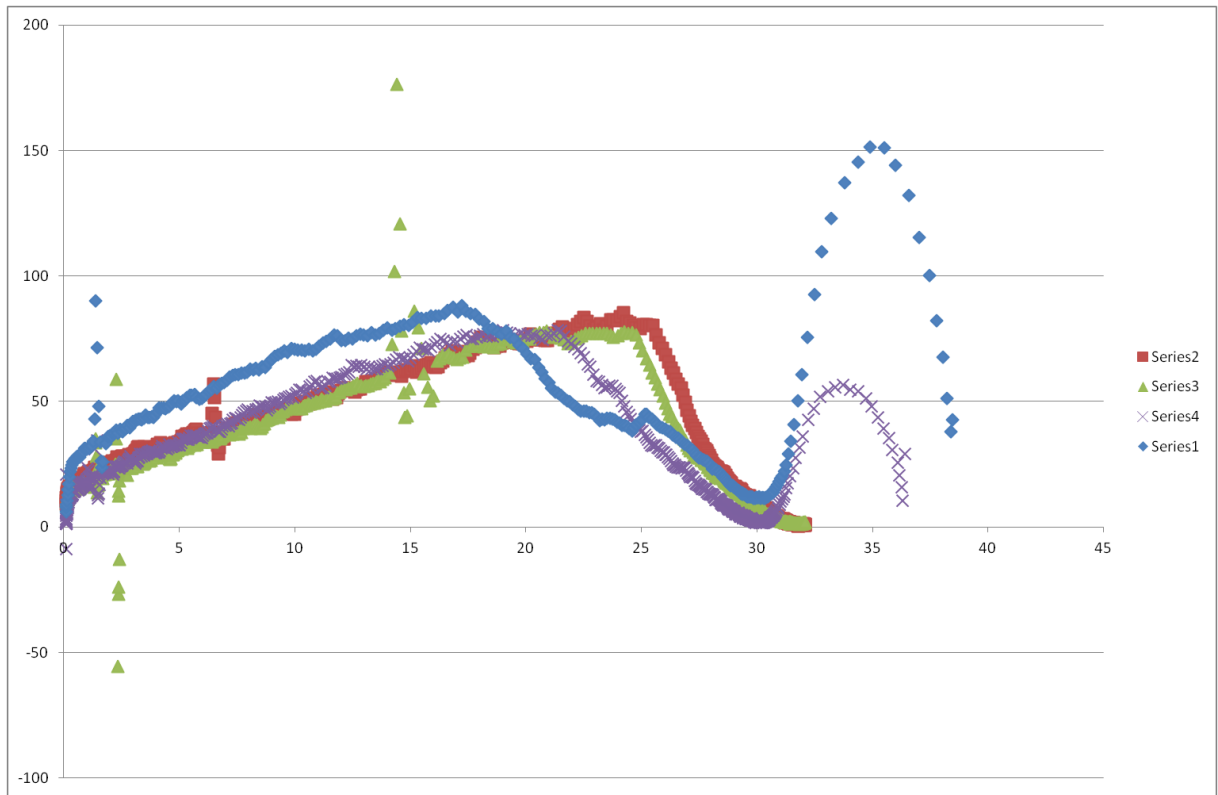


Fig 9. Elastic modulus. Mixtures OA:SA, 80:20 marro), 60:40 verd), 40:60 lila), 20:80 blau).

## State equations

### State equation

An analysis of the isotherms using the virial state equation has been done.

The plot of  $PA/(kT)$  vs  $P$  (Fig 10) can be adjusted with a polynomial de 2n degree,  $PA/(kT)=b_0+b_1P+b_2P^2$ , where  $b_0$ ,  $b_1$  and  $b_2$  are the virial coefficients.

The values of the viral coefficients are tabulated in table 1.

The following treatment can be applied to the mixture virial coefficients.

- $b_1)_m = b_1)_1 X_1^2 + b_1)_2 X_2^2 + 2b_1)_{12} X_1 X_2$
- $b_1)_m^{id} = b_1)_1 X_1 + b_1)_2 X_2$
- $b_1)^E = b_1)_m - b_1)_m^{id}$

The values of  $b_1)_{12}$  and  $b_1)^E$  are tabulated in Table 2 .

Results for  $b_1$  coef (Fig 11) indicate a gradual decrease from the OA to the SA. Similar occurs for the  $b_0$  coef. The higher value for  $b_1$  of OA is due to the higher repulsive interactions between molecules in this fatty acid in respect to the SA. The higher value for  $b_0$  of OA is due to a less degree of aggregation in this fatty acid in respect to the SA. The values of  $b_1)_m$  are in between those of the SA and OA, but higher than those of the straight line, that is the  $b_1)_E$  values are positive. This indicates more repulsive interactions in the mixture between SA and OA molecules, in respect to the separate components.

The values of  $b_1)_2$  are positive and higher than the mean value  $(b_1)_1 + (b_1)_2 / 2 = 0.09105$ , which also indicates more repulsion in the mixture between molecules.

The higher values of  $b_1)_2$  occurs when the content of OA is low, being higher than the value of  $b_1$  of pure OA. This fact can be explained because OA breaks the compactness of SA which results in an increase of the  $b_1$  coefficient (much more repulsion in respect to pure components).

**Table 1**

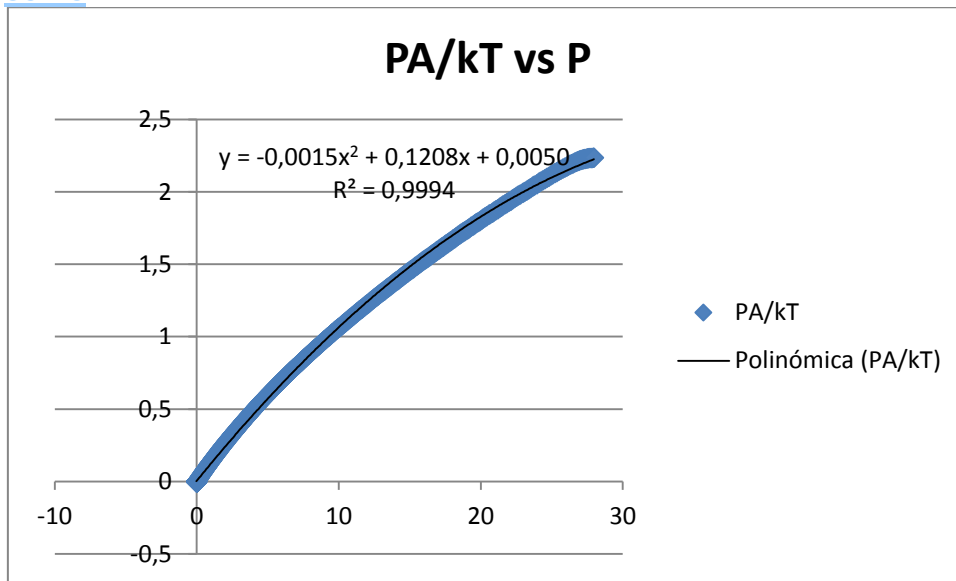
Virial coef	OA	80:20	60:40	40:60	20:80	SA
<b>B0</b>	<b>0.0055</b>	<b>0.0050</b>	<b>0.0046</b>	<b>0.0048</b>	<b>0.0007</b>	<b>-0.0021</b>
<b>B1</b>	<b>0.1255</b>	<b>0.1208</b>	<b>0.1080</b>	<b>0.1064</b>	<b>0.0883</b>	<b>0.0566</b>
<b>B2</b>	<b>-0.0015</b>	<b>-0.0015</b>	<b>-0.0014</b>	<b>-0.0013</b>	<b>-0.0011</b>	<b>-0.00018</b>
<b>R2</b>	<b>0.9994</b>	<b>0.9994</b>	<b>0.9994</b>	<b>0.9997</b>	<b>0.9999</b>	<b>0.9974</b>

**Table 2**

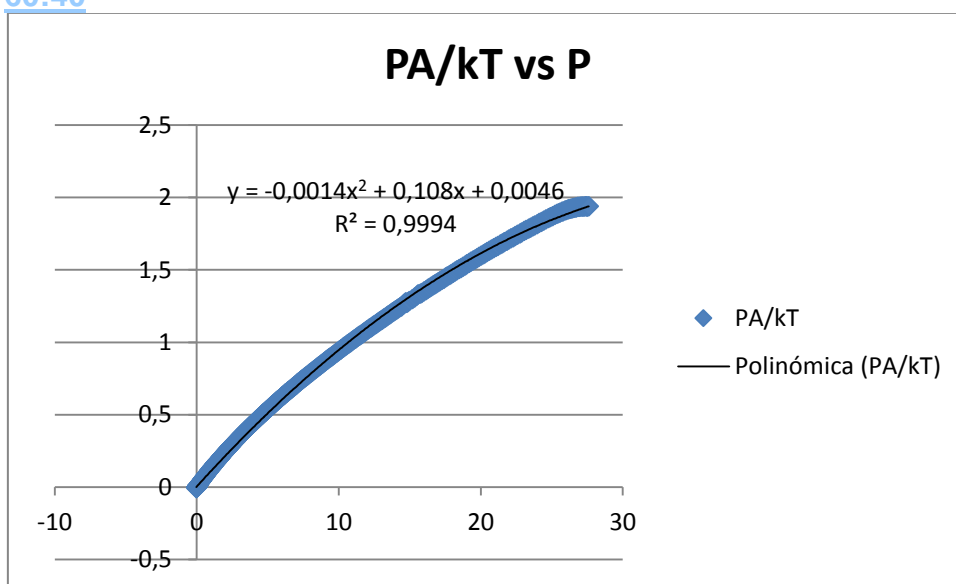
X(OA)	$b_1$	$b_1)_2$	$b_1)_E$
0	0,0566		0
0,217	0,0883	0,14033669	0,0167487
0,425	0,1064	0,13302954	0,0205175
0,625	0,108	0,10883667	0,0083375
0,816	0,1208	0,1176165	0,0079776
1	0,1255		0

OA:SA

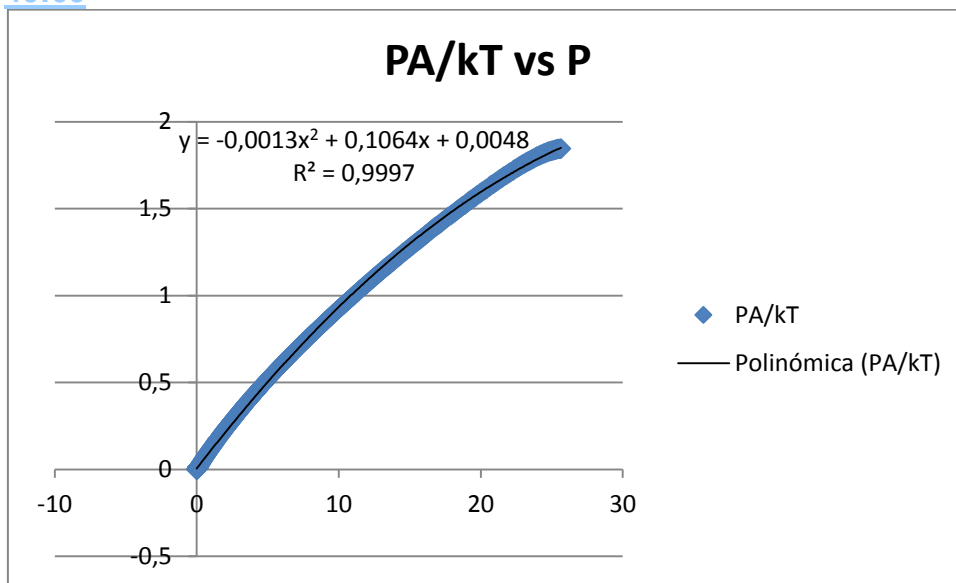
80:20



60:40



40:60



20:80

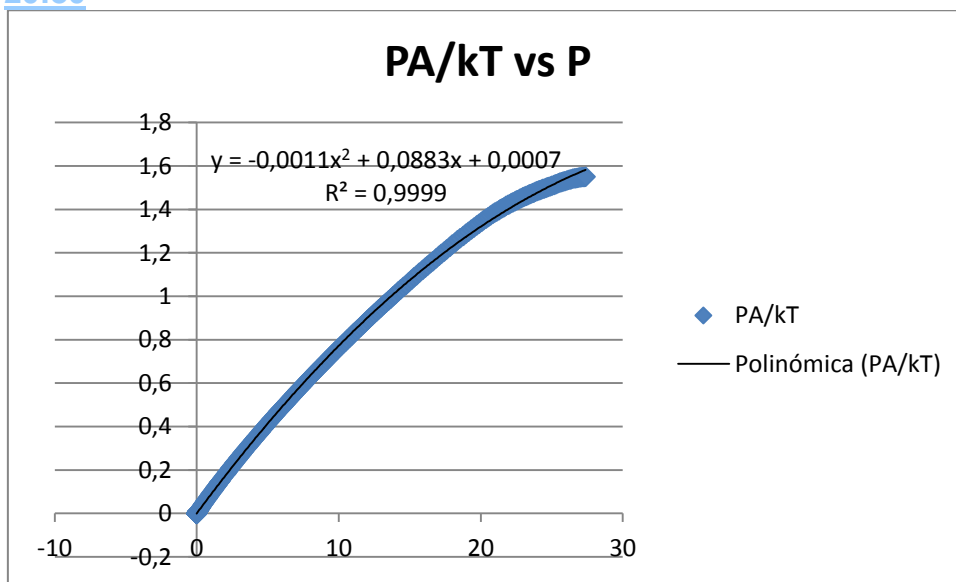
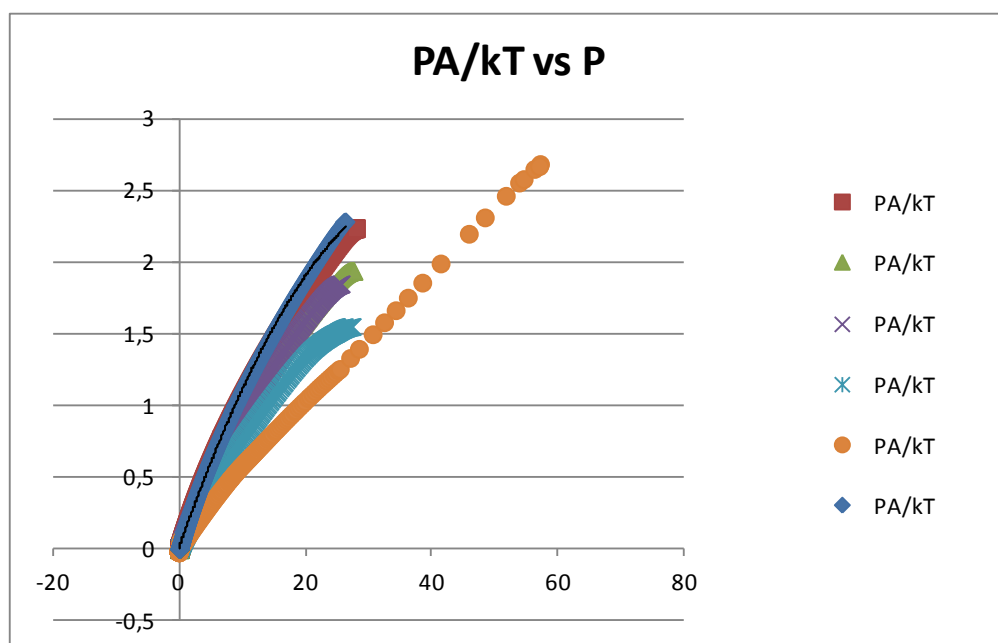


Fig 10. State equation plots for SA-OA mixtures.

**Fig 10b. Plots of  $(\Pi A/kT)$  vs  $\Pi$  for the several studied compositions SA-OA. (mixture + individuals)**



blau: oleic

groc:  
estearic

roig 80:20

verd 60:40

lila 40:60

cian 20:80

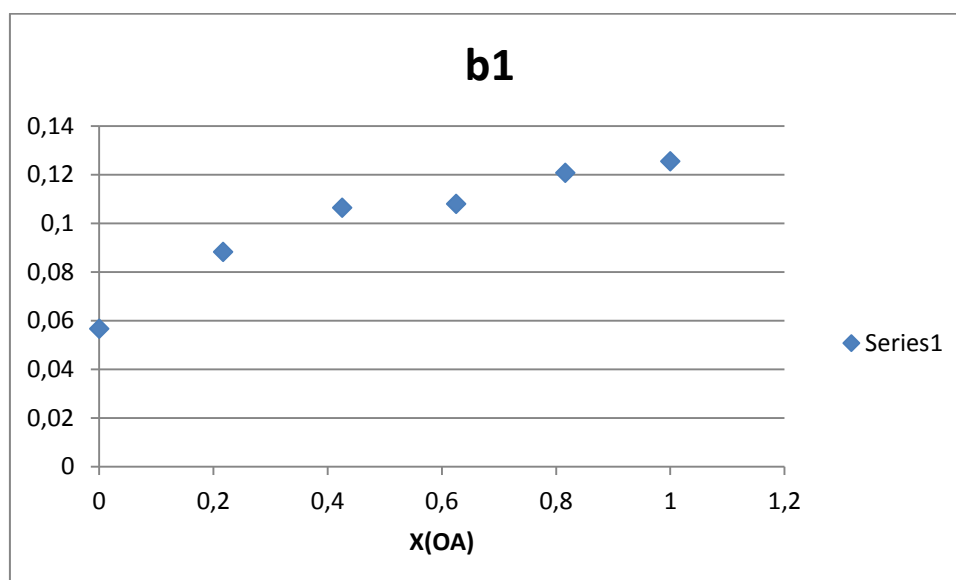


**Fig 11. Values of  $b1)m$  for mixtures of OA and SA.**

## AFM Mezclas.

To see the nanometric structure of the mixed monolayers, these have been transferred to mica using the Langmuir-Blodgett technique and AFM images have been done. Fig shows the topographic AFM images for a mixture with 80% of OA at two surfaces pressures of 5 and 22 mN/m. Images shows the presence of two separated phases, with rounded domains of higher height corresponding to SA. The saturated fatty acid, SA, forms more compact states with a lower molecular tilting and consequently higher height.

### Ácido oleico y ácido esteárico (AOL+AE)

En este caso, se hicieron LB a las presiones de 5 y 22 mN/m con la disolución con las proporciones 80% de AOL y 20% de AE. **(crec error ja que jo tinc 80 estearic i 20 d'oleic. A mes aquesta es mes congruent amb les arees dels dominis de AFM tenint en compte les arees individuals: estearic 2 nm a p=22 i oleic 4 nm, pertant  $2 \cdot 8 = 1.6$  i  $4 \cdot 0.2 = 0.8$ , es dir el doble d'estearic que de oleic. A mes part de l'estearic pot estar dissolt en l'oleic i per tant no arribarà al doble. Analitzar afm a 5 i 22 mN/m).**

Podemos ver que para las dos presiones, hay dos sustancias diferentes, es decir que los dos lípidos no se mezclan bien, lo que confirma lo que se ha dicho en la parte precedente.

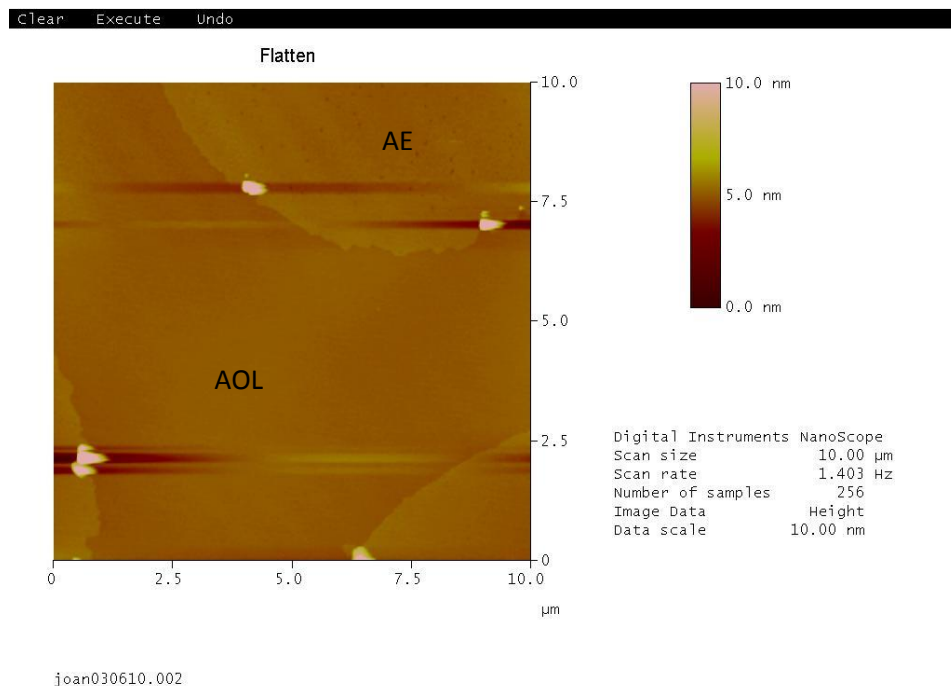


**Fig.12a. AFM-AOL+AE**



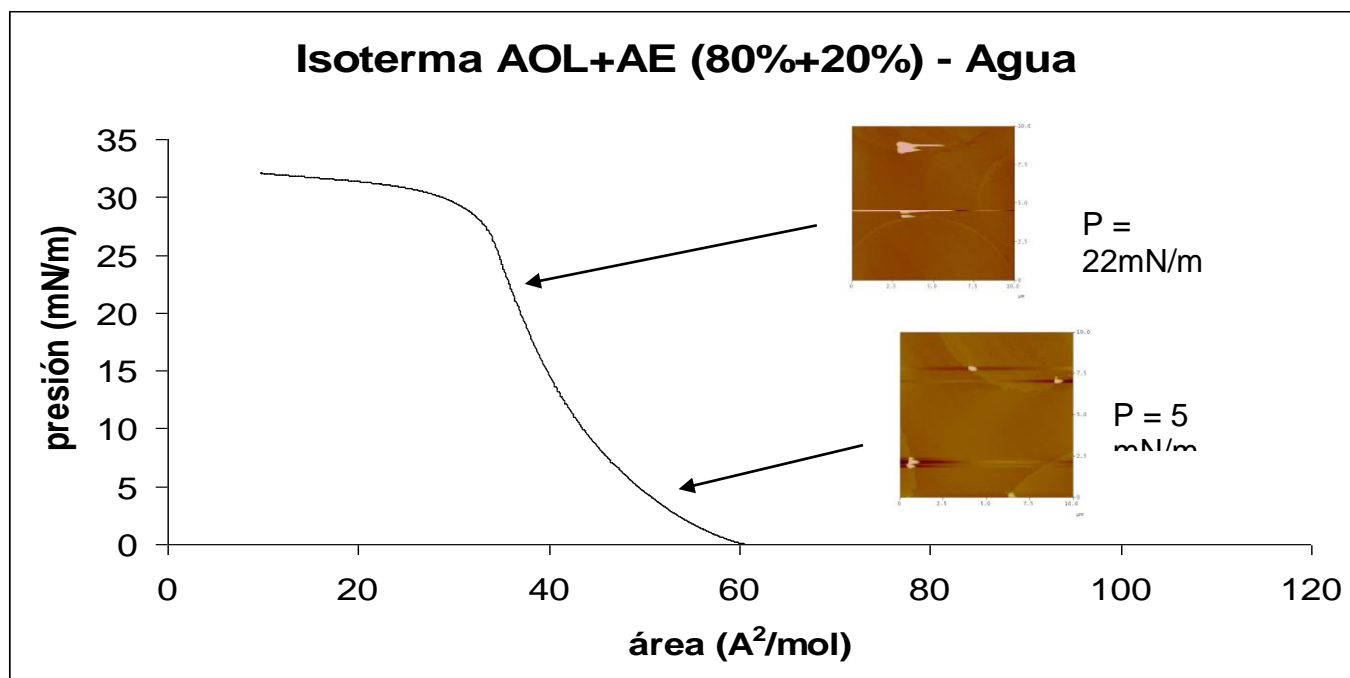
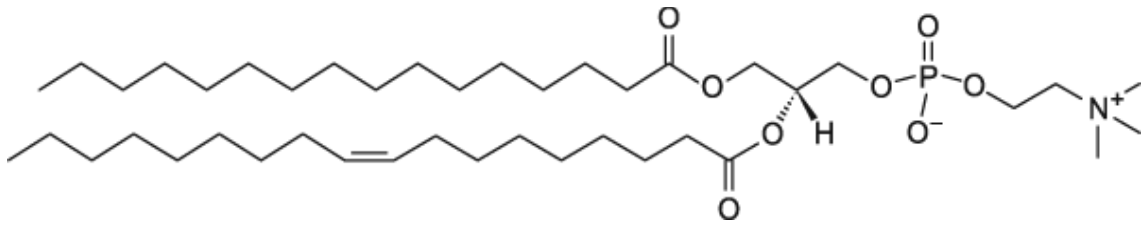
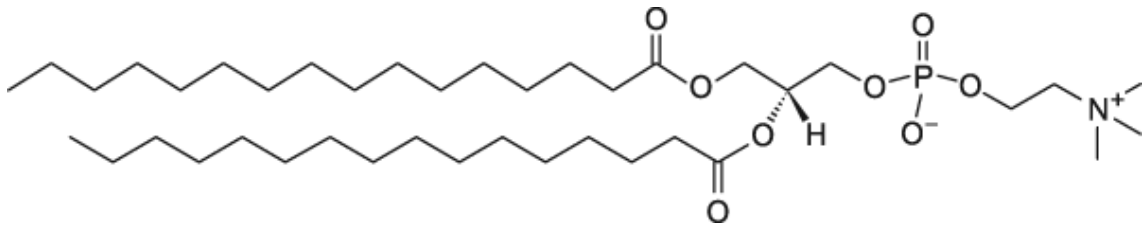


Figura 12b. Isoterma con imágenes de AFM, a 5 y 22 mN/m, para la mezcla AOL:AE 80:20.

## 2 DPPC-POPC



POPC



DPPC

## Isotherms

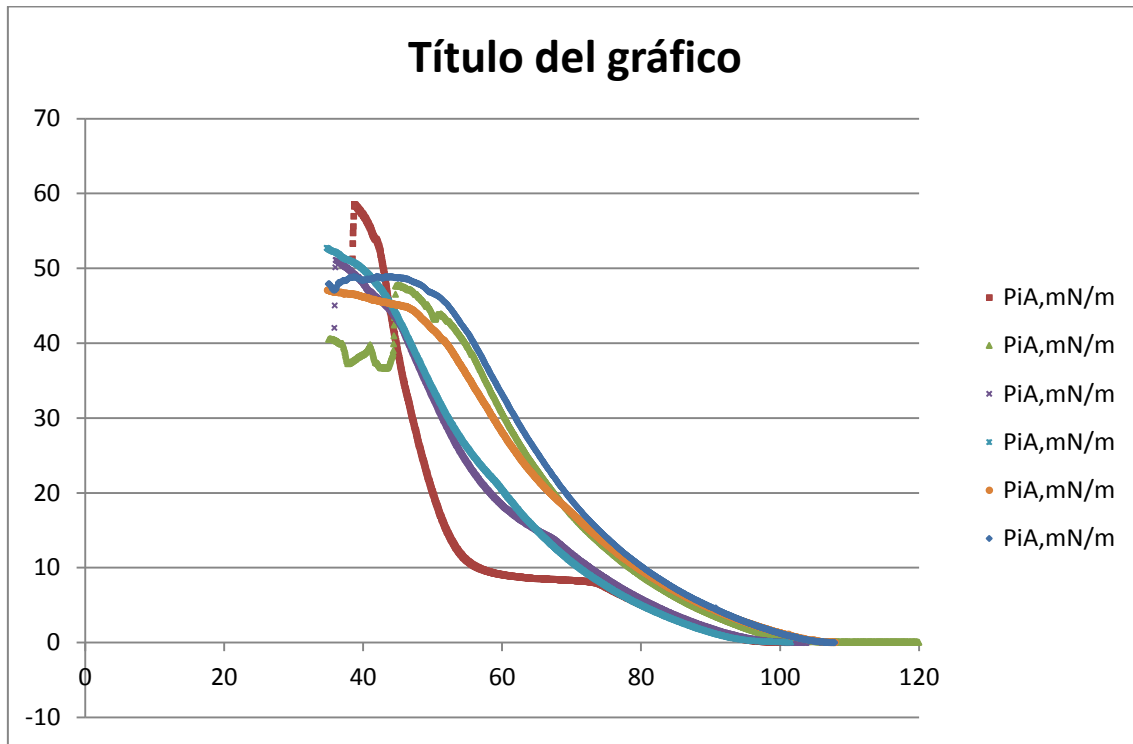


Fig 13. Isotherms of DPPC (red), POPC (blue) and DPPC-POPC mixtures (violet, cyan, orange, green).

Fig13 shows the isotherms of DPPC, POPC and DPPC-POPC mixtures.

For DPPC it is not observed a significant influence of the subphase (water, saline solution or saline+phosphate solution) in the isotherm.

On the other hand, it is not observed a significant influence of the compression rate ( $v=25$  o  $50 \text{ cm}^2/\text{min}$ ) on the isotherms.

- POPC victor surt una mica different al del Oscar pero es que la subfase es different (Oscar: NaCl+TRIS, Victor: aigua) I també la dissolució de preparació del POPC es different (Oscar: chloroform + methanol, Victor: chloroform).
- En insaturats la influencia de la subfase s major.

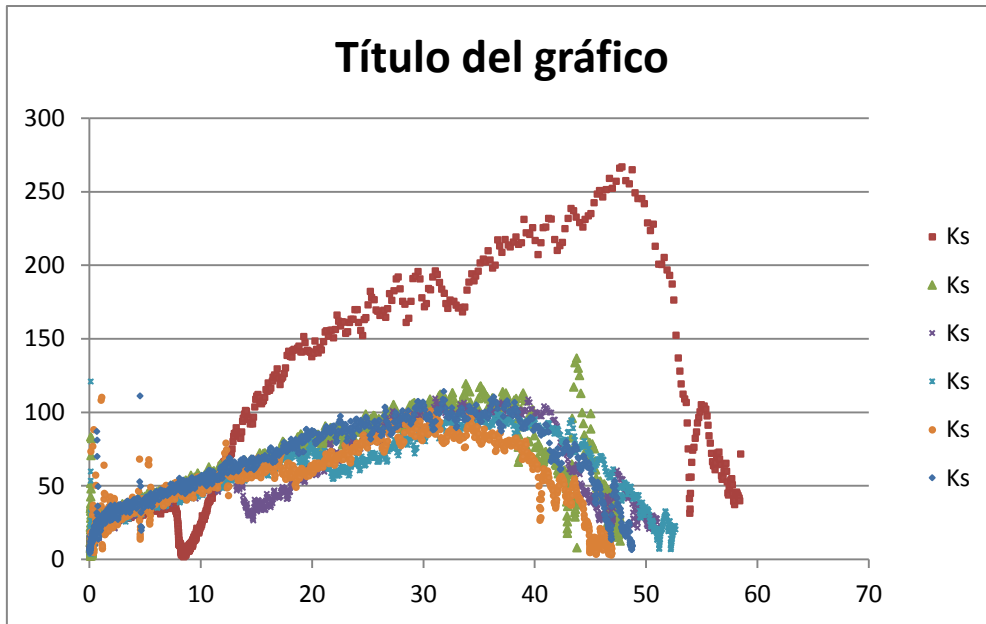


Fig 14. Elastic modulus of DPPC, POPC and DPPC-POPC mixtures.

Fig 14 shows the inverse of the compressibility coefficient (the elastic modulus) of DPPC, POPC and DPPC-POPC mixtures, obtained from the isotherms of Fig using the equation . DPPC presents a phase change from LE to LC at P around 8 mN/m, and POPC only presents LE state. Mixtures DPPC-POPC studied only presents LE state, with an inflexion at high DPPC contents, and with the inflexion P that increase when the DPPC content decreases.

Fig 15 shows the area per molecule vs the POPC molar fraction, at several P. It is observed in general positive deviations respect to the ideal case (straight line), but at low and high P the mixture with  $X(\text{POPC})=0.4$  present negative deviations which indicate less repulsive interactions or more attractive interactions (favorable interactions in respect to the individual components). This fact will be commented later.

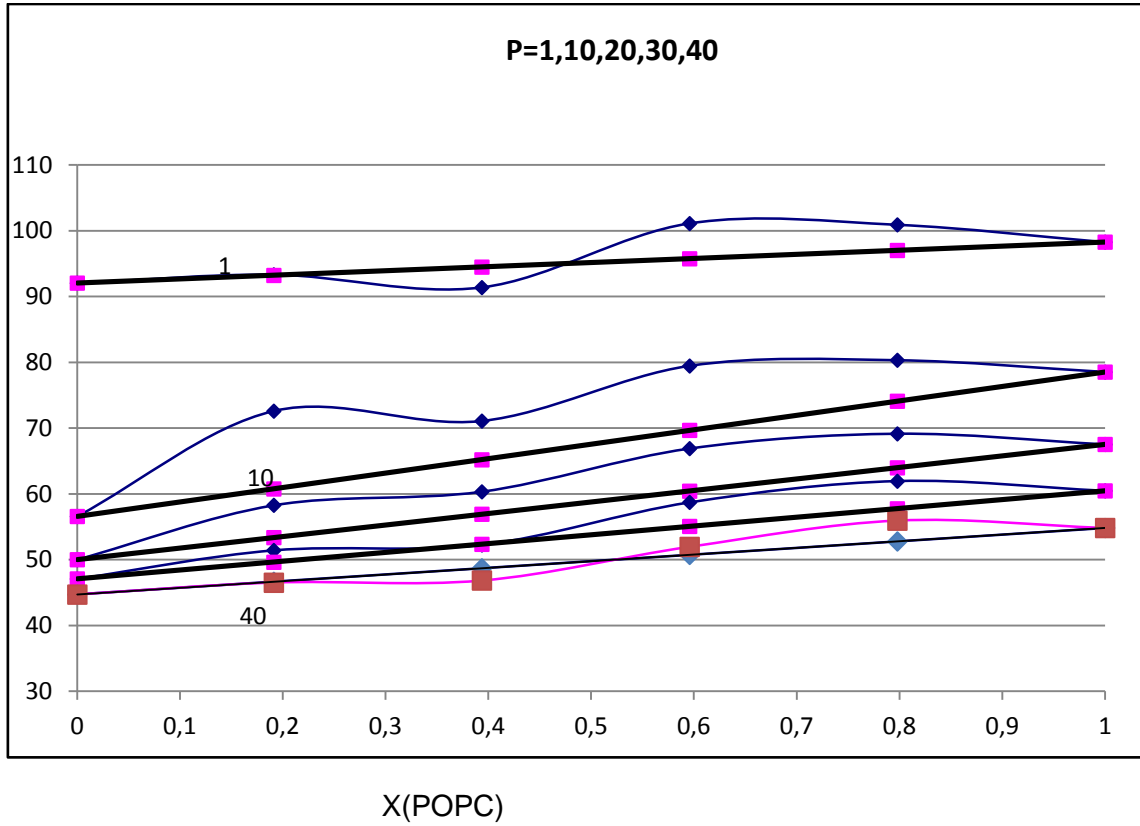


Fig 15. Area per molecule vs the POPC molar fraction, at several surface pressures(P).

### State equations

#### State equation

An analysis of the isotherms using the virial state equation has been done.

The plot of  $PA/(kT)$  vs  $P$  can be adjusted with a polynomial de  $2n$  degree,  
 $PA/(kT)=bo+b1P+b2P^2$ , where  $bo$ ,  $b1$  and  $b2$  are the virial coefficients.

Fig 16 shows the plot of  $PA/kT$  vs  $P$  and Table 3 summarizes the values of the virial coefficients obtained from the fitting.

**The following treatment can be applied to the mixture virial coefficients.**

- $b1)_m=b1)_1X_1^2+b1)_2X_2^2+2b1)_12X_1X_2$
- $b1)_m^{id}=b1)_1X_1+b1)_2X_2$
- $b1)_m^E=b1)_m-b1)_m^{id}$

The values of  $b1)_12$  and  $b1)_m^E$  are tabulated in Table 4.

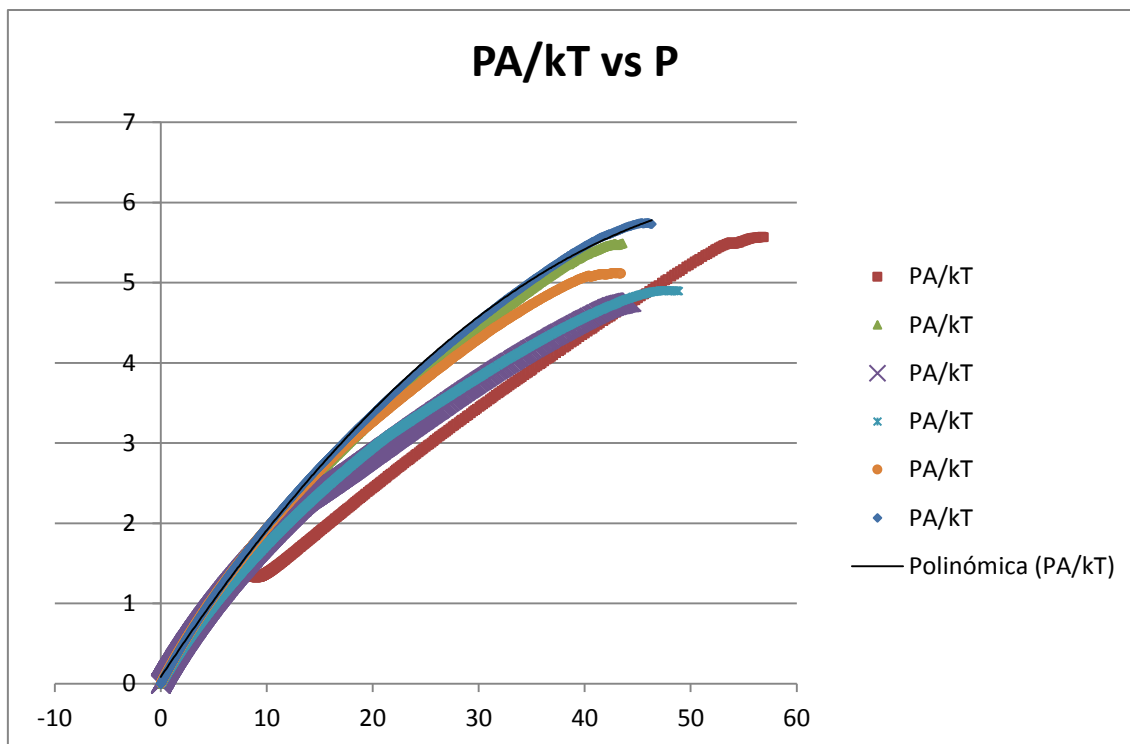


Fig 16. Plots of PA/kT vs P.

Table 3.

Virial coef	POPC	POPC 80	POPC 60	POPC 40	POPC 20	DPPC
B0	0.0319	0.0856	0.0923	0.0832	0.0978	0.1930
B1	0.2002	0.1991	0.1984	0.1744	0.1736	0.1333
B2	-0.0017	-0.0016	-0.0019	-0.0016	-0.0016	-0.00068
R2	0.9994	0.9995	0.9992	0.9989	0.9970	0.9916

Table 4.

X(POPC)	b1	b1)12	b1)E
0	0,1333		0
0,191	0,1736	0,256	0,0275
0,394	0,1744	0,198	0,0147
0,596	0,1984	0,219	0,0252
0,798	0,1991	0,205	0,0124
1	0,2002		0

It is seen from the table that b1 increases with the POPC content. This indicates more repulsive interactions for POPC and that the presence of POPC in the DPPC matrix also increases the repulsive interactions between molecules, in respect to DPPC molecules. The value of b0 for DPPC is lower than that of DPPC, indicating more aggregation in POPC than in DPPC (això sembla una mica estrany però podria ser degut a la major cadena del oleoil, encara que sigui insaturada).

Results for  $b_1$  coef (Fig 17) indicate a gradual decrease from the POPC to the DPPC. The higher value for  $b_1$  of POPC is due to the higher repulsive interactions between molecules in this fatty acid in respect to the DPPC. The higher value for  $b_0$  of OA is due to a less degree of aggregation in this fatty acid in respect to the SA. The values of  $b_1)_m$  are in between those of the DPPC and POPC, but higher than those of the straight line, that is the  $b_1)_E$  values are positive. This indicates more repulsive interactions in the mixture between DPPC and POPC molecules, in respect to the separate components. The values of  $b_1)_2$  are positive and higher than the mean value  $(b_1)_1 + (b_1)_2)/2 = 0.1667$ , which also indicates more repulsion in the mixture between molecules.

The higher values of  $b_1)_2$  occurs when the content of POPC is low, being higher than the value of  $b_1$  of pure POPC, except that of  $X(\text{POPC}) = 0.4$ . This fact can be explained because POPC breaks the compactness of DPPC which results in an increase of the  $b_1$  coefficient (much more repulsion in respect to pure components). As has been seen previously, when  $X(\text{POPC}) = 0.4$  the excess area is negative which is in agreement with the fact that seen now that the  $b_1)_2$  is the low value for the mixture and being lower than that of pure POPC. Thus, the mixture with  $X(\text{POPC}) = 0.4$  is the most favorable of the mixtures.

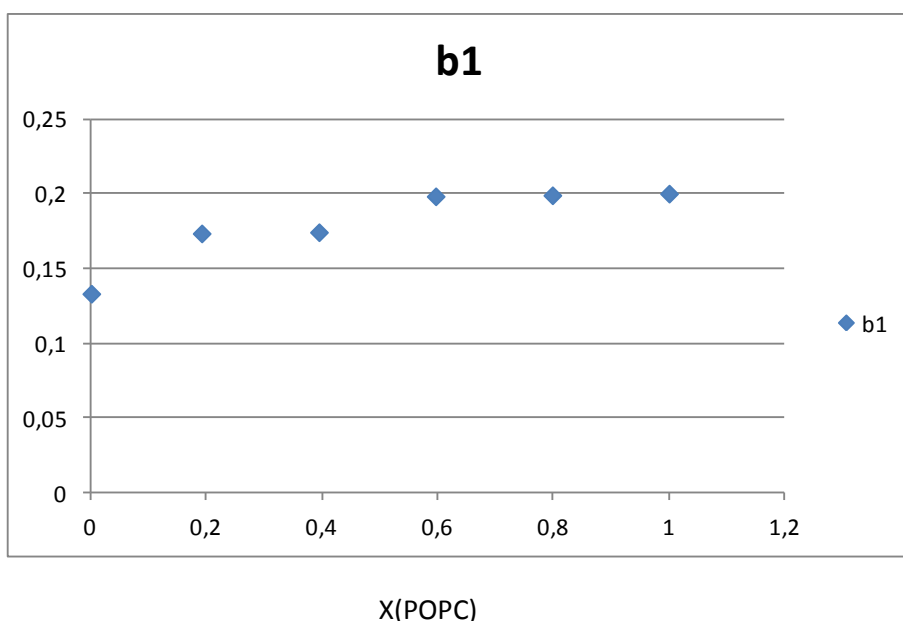


Fig 17. Values of  $b_1)_m$  for mixtures of DPPC and POPC.

## DISCUSSIÓ

Les isoterms indiquen que pot haverhi una certa miscibilitat entre components en ambdós casos, però que seria més gran en el cas dels fosfolipid que en els àcids grassos. L'anàlisi de  $A$  vs  $X$  indica aquesta miscibilitat però amb interaccions més desfavorables que per als components individuals. El fet que es produeixi miscibilitat s'ha d'atribuir a factors entropics. Aquestes interaccions desfavorables propicien la separació parcial de fases que s'observa en el sistema SA-OA a altes pressions i/o quan el contingut de SA és gran (en les isoterms o en imatges de afm). En el sistema DPPC/POPC fins i tot hi ha una composició ( $X_{\text{popc}}=0.4$ ) en que la mescla és favorable.

Les interaccions desfavorables poden deure's, en part a la presència de la insaturació.

Els valors de compressibilitat en les mescles s'assemblen més al del component més fluid (OA or POPC). EL COMPORTAMENT DE LES CORBES DE COMPRESSIBILITAT a P altes ES DIFERENT ALS DOS SISTEMES. EL QUE S'OBSERVA PER AL DPPC-POPC ES UN SOL MÀXIM, I AIXO ES DIFERENT A L'OBSERVAT PEL SA-OA JA QUE ALLÍ SI QUE APAREIXEN DOS MÀXIMS, I UNA CLARA FASE AMB SA, MENTRE QUE PER AL DPPC-POPC NO.

EN L'ANÀLISI DELS COEF DEL VIRIAL ES SIMILAR EN ELS DOS SISTEMES, JA QUE ELS VALORS DE  $B_1$  ESTAN ENTRE ELS DELS COMPONENTS INDIVIDUALS.

Quan  $x(\text{OA})=0.4$  hi ha interaccions desfavorables, més desfavorables, en canvi amb  $X(\text{POPC})=0.4$  són favorables.



## REFERENCES

Revisio bibliografica

Articles acid gras I relacionats, concret SA, OA

Mescles

Mescles saturat-insaturat, concret SA.OA

Articles fosfolipids I relacionats, concret DPPC, POPC

Mescles, mescles saturat-insaturat, concret DPPC-POPC

Articles acid gras - fosfolipid

### General

[Petty 1996] M.C. Petty, Langmuir-Blodgett Films, An Introduction, Cambridge University Press, Cambridge, 1996.

[Ulman 1990] A. Ulman, An Introduction to Ultrathin Organic Films, Academic Press, Boston, 1990.

[Richardson 2000] Functional organic and polymeric materials : molecular functionality-macroscopic reality / edited by Tim H. Richardson, Chichester : Wiley, cop. 2000.

### Articles acid gras o relacionat

1.

**Baba et al** (Teruhiko Baba, Katsuki Takai, Toshiyuki Takagi, Toshiyuki Kanamori, *Chemistry and Physics of Lipids* 172– 173 (2013) 31– 39. Effect of perfluoroalkyl chain length on monolayer behavior of partially fluorinated oleic acid molecules at the air–water interface)

A series of oleic acid (OA) analogs containing terminal perfluoroalkyl groups (CF<sub>3</sub>, C<sub>2</sub>F<sub>5</sub>, n-C<sub>3</sub>F<sub>7</sub>, n-C<sub>4</sub>F<sub>9</sub> or n-C<sub>8</sub>F<sub>17</sub>) was synthesized to clarify how the fluorinated chain length affects the stability and molecular packing of liquid-expanded OA

monolayers at the air–water interface. Although the substitution of terminal CF<sub>3</sub> group for CH<sub>3</sub> in OA had no effect on monolayer stability, further fluorination led to a gradual increase in monolayer stability at 25 °C. Surface pressure–area isotherm revealed that partially fluorinated OA analogs form more expanded monolayers than OA at low surface pressures, and that the monolayer behavior of OA analogs with the even-carbon numbered fluorinated chain is almost the same as that of OA upon monolayer compression, whereas the behavior of OA analogs with the odd-carbon numbered fluorinated chain significantly differs from that of OA. These results indicate: (i) the terminal short part (at least C<sub>2</sub> residue) in OA predominantly determines the liquid-expanded monolayer stability; (ii) the molecular packing state of OA may be perturbed by the substitution of a short odd-carbon numbered fluorinated chain; (iii) hence, OA analogs with even-carbon numbered chain are considered to be preferable as hydrophobic building blocks for the synthesis of fluorinated phospholipids.

#### **MOLT interessant**

Barzyk and Vuorinen (W Barzyk, J Vuorinen, *Colloids Surf A* 385 (2011) 1-10. Application of the vibrating plate technique to measuring electric surface potential,  $\Delta V$ , of solutions; the flow cell for simultaneous measurement of the  $\Delta V$  and the surface pressure) studied the surface films of n-decanoic acid, n-decyl-trimethylammonium bromide and sodium n-dodecyl sulphate.

Dhathathreyan (A Dhathathreyan, *Colloids Surf A* 318 (2008) 307-314. Dissociation constants of long-chain hydroxy fatty acids in Langmuir-Blodgett films) measured the effect of –OH groups on the pK values of hydroxyl fatty acids, and obtained the surface pressure-area isotherms and BAM images of the films.

Dupres et al (V Dupres, S Cantin, F Benhabib, F Perrot, P Fontaine, M Goldmann, J Daillant, O Konovalov, *Langmuir* 19 (2003) 10808-10815. Superlattice formation in fatty acid monolayers on a divalent ion subphase: Role of chain length, temperature, and subphase concentration) used behenic acid to study the influence of several factors on the Langmuir monolayer formation.

Kenn et al (R. M. Kenn, C. Biihm, A. M. Bib, I. R. Peterson, H. Mohwald, J. Als-Nielsen, and K. Kjaer, *J. Phys. Chem.* (1991),95,2092-2097. Mesophases and Crystalline Phases In Fatty Acid Monolayers) investigated The polymorphism in docosanoic (behenic) acid monolayers at the air/water interface by means of X-ray Diffraction.

Kundu and Raychaudhuri (S Kundu and AK Raychaudhuri, *J Colloid Interf Sci* 353 (2011) 316-321. Effect of water and air-water interface on the structural modification of Ni-arachidate Langmuir-Blodgett films) studied the deposition on hydrophilic Si substrates of Ni-arachidate films from the air-water interface.

Kundu (S Kundu, Colloids Surf A 317 (2008) 618-624. Langmuir-Blodgett film from a bi-molecular layer at air-water interface) used ferric stearate to form LB films on hydrophilic silicon.

Lundgren SM et al (SM Lundgren, M Ruths, K Danerlov, K Persson, J Colloid Interf Sci 326 (2008) 530-536. Effects of unsaturation on film structure and friction of fatty acids in a model base oil) studied the normal and friction forces between monolayers of three fatty acids (stearic, oleic and linoleic acid) and a rosin acid (dehydroabietic acid) using a surface forces apparatus.

Mildner and Dynarowicz-Latka (J Mildner and P Dynarowicz-Latka, Colloids Surf B 90 (2012) 244-247. B-Carotene does not form a true Langmuir monolayer at the air-water interface) discussed the ability of b-carotene to form Langmuir monolayers using surface pressure-area isotherms and BAM.

**Maheshwari** and Dhathathreyan (R. Maheshwari and A. Dhathathreyan, Journal of Colloid and Interface Science 275 (2004) 270–276. Influence of ammonium nitrate in phase transitions of Langmuir and Langmuir–Blodgett films at air/solution and solid/solution interfaces) studied the effect of ammonium nitrate on the phase transitions in Langmuir films of amphiphiles—stearic acid, stearyl amine (STAM), stearyl alcohol, dihexadecylphosphate, and the quarternized ammonium salt dioctadecyldimethylammonium bromide at air/water interface and in local ordering of their Langmuir–Blodgett films (LB films).

Snow et al (Arthur W. Snow, Glenn G. Jernigan, Mario G. Ancona, [Thin Solid Films 556 \(2014\) 475–484](#). Equilibrium spreading pressure and Langmuir–Blodgett film formation of omega-substituted palmitic acids) measured Langmuir–Blodgett isotherms and equilibrium spreading pressures for compounds of the series  $X-(CH_2)_{15}COOH$ ,  $X = CH_3, SH, OH, F, Cl, Br$ . Only the  $CH_3$  and  $F$  terminated compounds formed monolayers with sufficient stability for accurate isotherm measurement, film transfer and X-ray photoelectron spectroscopic analysis.

Yang et al (G Yang, X Jiang, S Dai, G Cheng, X Zhang, Z Du, Thin Solid Films 518 (2010) 7086-7092. Morphology, defect evolutions and nano-mechanical anisotropy of behenic acid monolayer) prepared LB films of behenic acid and their morphological evolutions and nano-mechanical anisotropy were studied by AFM and LFM.

## 2. Mixed

Broniatowski and Dynarowicz-Latka (M Broniatowski and P Dynarowicz-Latka, Langmuir 22 (2006) 2691-2696. Semifluorinated chains at the air/water interface:

studies of the interaction of a semifluorinated alkane with fluorinated alcohols in mixed Langmuir monolayers) studied mixtures of semifluorinated henicosatriacontane with fluorinated alcohols, using surface pressure-area isotherms and BAM.

Brzozowska et al (A.M. Brzozowska, F. Mugele, M.H.G. Duits, [Colloids and Surfaces A: Physicochem. Eng. Aspects](#) 433 (2013) 200–211. Stability and interactions in mixed monolayers of fatty acid derivatives on Artificial Sea Water) studied the formation and stability of fatty acid and derivatives films on aqueous sub-phases by means of Langmuir trough experiments. Films were prepared from pure stearic acid (SA), stearyl amine (SAm) and 12-phenyldodecanoic acid (PDA), and from binary systems of SA with either SAm or PDA. For the aqueous sub-phase, multicomponent salt solutions ('Artificial Sea Water') at various concentrations (cASW, 0–100%) and pH values (3–7) were explored.

Eftaiha and Paige (A F. Eftaiha, M F. Paige, [Journal of Colloid and Interface Science](#) 380 (2012) 105–112. Phase-separation of mixed surfactant monolayers: A comparison of film morphology at the solid–air and liquid–air interfaces) examined the morphologies of phase-separated monolayer films prepared from two different binary mixtures of perfluorocarbons and hydrocarbons have been examined and compared, for the first time, at the solid–air and liquid–air interfaces. Films were comprised of binary mixtures of arachidic acid (C<sub>19</sub>H<sub>39</sub>COOH) with perfluorotetradecanoic acid (C<sub>13</sub>F<sub>27</sub>COOH) and of palmitic acid (C<sub>15</sub>H<sub>31</sub>COOH) with perfluorooctadecanoic acid (C<sub>17</sub>F<sub>35</sub>COOH).

Ekelund et al (K Ekelund, E Sparr, J Engblom, H Wennerström, S Engström, *Langmuir* 15 (1999) 6946-6949. An AFM study of lipid monolayers. 1. Pressure-induced phase behavior of single and mixed fatty acids) transferred mixed films of palmitic (C<sub>16</sub>:0) and lignoceric (C<sub>24</sub>:0) acid to a mica substrate and observed them by AFM.

Imae et al (T Imae, T Takeshita, M Kato, *Langmuir* 16 (2000) 612-621. Phase separation in hybrid Langmuir-Blodgett films of perfluorinated and hydrogenated amphiphiles. Examination by AFM) investigated the phase separation of eicosanoid acid and perfluorocarboxylic acids by using AFM and surface pressure-area isotherms.

Kurnaz and Schwartz (ML Kurnaz and DK Schwartz, *J Phys Chem* 100 (1996) 11113-11119. Morphology of microphase separation in arachidic acid-cadmium arachidate LB multilayers) studied the deposition of LB films of arachidic acid from a dilute CdCl<sub>2</sub> subphase at different pH.

Matsumoto et al (M Matsumoto, K-I Tanaka, R Azumi, Y Kondo, N Yoshino, *Langmuir* 19 (2003) 2802-2807. Structure of phase-separated LB films of hydrogenated and perfluorinated carboxylic acids investigated by IR spectroscopy, AFM and FFM)

investigated the structure of mixed Langmuir and LB films of arachidic acid and perfluorotetradecanoic acid.

Matsumoto et al (M Matsumoto, K-I Tanaka, R Azumi, Y Kondo, N Yoshino, *Langmuir* 20 (2004) 8728-8734. Template-directed patterning using phase-separated LB films) investigated the structure of mixed LB films of conventional amphiphiles and amphiphilic perfluorinated silane-coupling agents and determined the phase-separated domains.

Qaqish and Paige (SE Qaqish and MF Paige, *J Colloid Interf Sci* 325 (2008) 290-293. Characterization of domain growth kinetics in a mixed perfluorocarbon-hydrocarbon Langmuir-Blodgett monolayer) performed mixed LB films of arachidic acid and perfluorotetradecanoic acid and using AFM studied the domain formation.

Seoane et al (R Seoane, P Dynarowicz-Latka, J Miñones Jr, I Rey, *Colloid Polym Sci* 279 (2001) 562-570. Mixed Langmuir monolayers of cholesterol and essential fatty acids) investigated Langmuir monolayers of cholesterol and various fatty acids, such as stearic, oleic, linoleic, linolenic and arachidonic acids, spread at the air/water interface.

Seoane et al (R Seoane, J Miñones, O Conde, J Miñones Jr, M Casas, E Iribarnegaray, *J Phys Chem B* 104 (2000) 7735-7744. Thermodynamic and BAM studies of fatty acid-cholesterol mixtures at the air-water interface) spread mixtures of cholesterol with stearic (STA), oleic (OA), and linoleic (LA) acids as monolayers at the air/water interface and were used as model systems to examine the hypocholesterolemic effect of fatty acids. Miscibility and interactions between the components of the cholesterol/fatty acid systems were studied basing on the analysis of surface pressure/area isotherms completed with Brewster angle microscopy images.

Torrent (OA-cholesterol) *Nanobioscience. J. Torrent-Burgués BioNanoSci.* (2011) 1:202–209

Oleamide (OA) and its mixtures with other lipids are of interest in some biological systems, such as the tear film or the cerebrospinal fluid. In this work, the behavior of OA, OA–dipalmitoylphosphatidylcholine (DPPC), and OA–cholesterol films is studied using surface pressure–area isotherms and atomic force microscopy, and analyzing the collapse pressure vs. composition, the compressibility, and the mean area vs. composition for several surface pressures. It is observed that OA forms homogeneous monolayers in a liquid-expanded state until the collapse surface pressure and the mixing with DPPC and cholesterol. The collapse surface pressure changes with the mixture composition, and in the case of DPPC, a noticeable influence of OA in the liquid-expanded/liquid-condensed phase change of DPPC is observed. The excess area is positive for the OA/DPPC films, but mostly negative for the OA–cholesterol films. These results are of interest for the target of formulation of artificial tears containing lipids.

Watanabe et al (S Watanabe, R Okuda, R Azumi, H Sakai, M Abe, J Colloid Interf Sci 363 (2011) 379-385. Effect of subphase temperature on the phase-separated structures of mixed Langmuir and Langmuir-Blodgett films of fatty acids and hybrid carboxylic acids) studied mixed films of several fatty acids and fluorinated carboxylic acids and determined the phase-separation behavior.

### 3. Mixed saturated – unsaturated fatty acids

**Feher** et al (Al Feher, FD Collins, TW Healy, Australian J Chem 30 (1977) 511-519. Mixed monolayers of simple saturated and unsaturated fatty acids) obtained surface pressure-area isotherms for single and binary films in the acid series, oleic, elaidic, stearic and arachidic.

**Ocko** et al (Benjamin M. Ocko, Michael S. Kelley, Ani T. Nikova and Daniel K. Schwartz, *Langmuir* **2002**, 18, 9810-9815. Structure and Phase Behavior of Mixed Monolayers of Saturated and Unsaturated Fatty Acids) used Grazing incidence X-ray diffraction (GIXD) and Brewster angle microscopy (BAM) to study the miscibility and phase behavior of Langmuir monolayers composed of a mixture of a saturated (stearic) and a trans-monounsaturated (elaidic) fatty acid.

### Articles de fosfolipids I relacionats

Baba et al (Teruhiko Baba, Katsuki Takai, Toshiyuki Takagi, Toshiyuki Kanamori. Colloids and Surfaces B: Biointerfaces 123 (2014) 246–253. Effect of the fluorination degree of hydrophobic chains on the monolayer behavior of unsaturated diacylphosphatidylcholines bearing partially fluorinated 9-octadecynoyl (stearoyl) groups at the air–water interface)

The effect of the fluorination degree of hydrophobic chains on the monolayer behavior of unsaturated diacylphosphatidylcholines (PCs) was examined by employing a series of PCs bearing partially fluorinated 9-octadecynoyl (stearoyl) groups (DFnStPCs, n: the number of fluorinated carbon atoms in a stearoyl group; n = 1, 2, 4, 8), including their hydrophobic parts – partially fluorinated stearic acids (FnStAs) – at the air–water interface. —A isotherm measurements and Brewster angle microscope observations were done.

### MOLT interessant

Flasinski et al (Michał Flasinski, Paweł Wydro, Marcin Broniatowski, [Journal of Colloid and Interface Science](#) **418** (2014) 20–30. Lyso-phosphatidylcholines in Langmuir monolayers – Influence of chain length on physicochemical characteristics of single-chained lipids)

Single-chained phospholipids constitute a class of membrane components found in normal cells in relatively low concentration; however, these group of compounds are known owing to their broad physiological activities. Despite that the knowledge concerning fundamental physicochemical properties of lyso-lipids is very limited and in contrast to double-chained phospholipids there is an obvious deficiency of studies focused on correlation between their amphipathic character and film-forming properties with biological activities. In the present paper we have attempted to explain the main issues regarding the characteristics of lyso-PCs in monolayers at the air/aqueous interface.

Kaviratna and Banerjee (A.S. Kaviratna, R. Banerjee, *Colloids and Surfaces A: Physicochem. Eng. Aspects* **345** (2009) 155–162. The effect of acids on dipalmitoyl phosphatidylcholine (DPPC) monolayers and liposomes)

Dipalmitoyl phosphatidylcholine (DPPC) is the most abundant phospholipid in lung surfactant, primarily responsible for the reduction of surface tension to near 0mN/m during expiration. In addition, DPPC liposomes are also used for drug delivery. In this study, the effects of hydrochloric acid, nitric acid and sulphuric acid on various properties of DPPC was investigated. The surface pressure versus area isotherms of DPPC monolayers at different concentrations of acid were obtained using a Langmuir–Blodgett trough. Distinct changes in the shapes of DPPC isotherms were observed in presence of acid.

KLOPFER AND VANDERLICK (K. J. KLOPFER AND T. K. VANDERLICK

*JOURNAL OF COLLOID AND INTERFACE SCIENCE* **182**, 220–229 (1996). Isotherms of Dipalmitoylphosphatidylcholine (DPPC) Monolayers: Features Revealed and Features Obscured)

Pressure–area isotherms of dipalmitoylphosphatidylcholine (DPPC) exhibit a two-phase region wherein domains of a liquid-condensed (LC) phase are dispersed in the less ordered liquid- expanded (LE) phase. Fluorescence microscopy has been used over the past years to visualize the shapes displayed by DPPC domains throughout the coexistence region; characteristic domain shapes include those resembling dimpled beans and S-like figures. In this paper we show that the types and distributions of domain shapes formed throughout the coexistence region depend sensitively on the rate of monolayer compression

Park (Jin-Won Park, [Colloids and Surfaces B: Biointerfaces](#) **86** (2011) 166–168.

Curvature effect on nanometer-scale surface properties of phospholipid layers) formed Phospholipid bilayers through liposome fusion on surfaces with different curvatures that were defined with silica spheres deposited on silicon water. Prior to the fusion, the surfaces became hydrophobic with octadecyltrimethoxysilane solution. Using atomic force microscope, surface forces were measured on dipalmitoylphosphatidylcholine

(DPPC) layers and dioleoylphosphatidylcholine (DOPC) layers upon the curvature at 25 °C.

Rodríguez et al (Ma. Rosario Rodríguez Niño, Ana Lucero, Juan M. Rodríguez Patino, Colloids and Surfaces A: Physicochem. Eng. Aspects 320 (2008) 260–270. Relaxation phenomena in phospholipid monolayers at the air–water interface) studied long-term relaxation phenomena in dipalmitoyl phosphatidylcholine (DPPC) and dioleoyl phosphatidylcholine (DOPC) monolayers spread at the air–water interface as a function of the surface pressure and the aqueous phase pH (pH 5, 7, and 9). Long-term relaxation phenomena were determined in an automated Langmuir-type film balance at constant temperature (20 °C).

Weiss et al (Martin Weis, Wei Ou-Yang, Takahiro Aida, Tetsuya Yamamoto, Takaaki Manaka, Mitsumasa Iwamoto, Thin Solid Films 517 (2008) 1317–1320. Study of electrostatic energy contribution on monolayer domains size) studied phospholipid organic monolayer at the air–water interface in the presence of magnesium ions. For this reason the domain size by Brewster angle microscopy (BAM) as well as the Gibbs energy by thermodynamic analysis was evaluated.

Yang and Kleijn (Junlin Yang and J. Mieke Kleijn, Biophysical Journal Volume 76 January 1999 323–332. Order in Phospholipid Langmuir-Blodgett Layers and the Effect of the Electrical Potential of the Substrate) investigated the ordering in dipalmitoylphosphatidylcholine (DPPC) Langmuir-Blodgett monolayers and bilayers on a semiconducting indium tin oxide (ITO) surface at the equilibrium potential of the interface and at various externally applied potentials. Second- and fourth-rank order parameters of a diphenylhexatriene (DPH) containing phospholipid probe were derived from total internal reflection fluorescence measurements, and orientation distributions were calculated using the maximum-entropy method

## Mixed

Domenech et al (Nos COLSUB 2005) POPE-POPC. Surface thermodynamics study of monolayers formed with heteroacid phospholipids of biological interest  
O`scar Domenech, Juan Torrent-Burgues Sandra Merino, Fausto Sanz,  
M. Teresa Montero, Jordi Hern´andez-Borrell. Colloids and Surfaces B: Biointerfaces 41 (2005) 233–238

The interaction of 1-palmitoyl-2-oleoyl-*sn*-glycero-3-phosphocoline (POPC) and 1-palmitoyl-2-oleoyl-*sn*-glycero-3-phosphoethanolamine (POPE), two of the major components in biological membranes, were investigated using the monolayer technique at the air–water interface. The pressure–area isotherms indicate that both phospholipids are miscible through all range of compositions. POPE–POPC form stable mixtures, with a minimum for the Gibbs energy of mixing at XPOPC = 0.4. A virial equation of state was fitted to the experimental values.



Positive values found for the second virial coefficient indicate repulsion between POPC and POPE. The interaction parameter was evaluated which indicated that a corresponding decrease in the repulsion occurs when POPC molar fraction is low. This effect suggests the existence of hydrogen bonds between POPE and the water beneath the interface.

Domenech et al (Òscar Domènech, Fausto Sanz, M. Teresa Montero, Jordi Hernández-Borrell, *Biochimica et Biophysica Acta* 1758 (2006) 213–221. Thermodynamic and structural study of the main phospholipid components comprising the mitochondrial inner membrane)  
Cardiolipin (CL) is a phospholipid found in the energy-transducing membranes of bacteria and mitochondria and it is thought to be involved in relevant biological processes as apoptosis. In this work, the mixing properties of CL and 1-palmitoyl-2-oleoyl-sn-glycero-3-phosphocoline (POPC) and 1-palmitoyl-2-oleoyl-sn-glycero-3-phosphoethanolamine (POPE) at the air–water interface, have been examined using the thermodynamic framework analysis of compression isotherms

Dynarowicz-Łatka et al (Patrycja Dynarowicz-Łatka, Anita Wnetrzak, Marcin Broniatowski, Michał Flasiński, *Colloids and Surfaces B: Biointerfaces* 107 (2013) 43–52. Miscibility and phase separation in mixed erucylphosphocholine–DPPC Monolayers)  
Binary Langmuir monolayers composed of 1,2-dipalmitoyl-sn-phosphatidylcholine (DPPC) and erucylphosphocholine (ErPC) – a new generation anti-cancer drug of phospholipids-like structure, have been studied with classical Langmuir technique complemented with Brewster angle microscopy (BAM) and Grazing Incidence X-ray Diffraction (GIXD).

Garcia-manyes et al (Sergi Garcia-Manyes, Òscar Domènech, Fausto Sanz, M.Teresa Montero, Jordi Hernandez-Borrell, *Biochimica et Biophysica Acta* 1768 (2007) 1190–1198. Atomic force microscopy and force spectroscopy study of Langmuir–Blodgett films formed by heteroacid phospholipids of biological interest)

Langmuir–Blodgett (LB) films of two heteroacid phospholipids of biological interest 1-palmitoyl-2-oleoyl-sn-glycero-3-phosphoethanolamine (POPE) and 1-palmitoyl-2-oleoyl-sn-glycero-3-phosphocholine (POPC), as well as a mixed monolayer with  $\chi_{\text{POPC}}=0.4$ , were transferred onto mica in order to investigate by a combination of atomic force microscopy (AFM) and force spectroscopy (FS) their height, and particularly, their nanomechanical properties.

Hac-Wydro et al (Katarzyna Hac-Wydro, Michał Flasiński, Marcin Broniatowski, Patrycja Dynarowicz-Łatka, Jarosław Majewski, *Journal of Colloid and Interface Science* 364 (2011) 133–139. Properties of b-sitostanol/DPPC monolayers studied with Grazing Incidence X-ray Diffraction (GIXD) and Brewster Angle Microscopy

Although the influence of structurally modified sterols on artificial membranes has been intensively investigated, studies on the properties of stanols, which are saturated analogs of sterols, are very rare. Therefore, we have performed Grazing Incidence X-ray Diffraction (GIXD) experiments aimed at studying in-plane organization of a plant stanol– $\beta$ -sitostanol monolayer and its mixtures with 1,2-dipalmitoyl-sn-glycero-3-phosphocholine – DPPC at the air/water interface. The collected GIXD data, resulting in-plane parameters and BAM images provide information on molecular organization and in-plane ordering of the investigated films.

Hac-Wydro et al (Katarzyna Hac-Wydro, Michał Flasiński, Paweł Wydro, Patrycja Dynarowicz-Łatka, [Colloids and Surfaces B: Biointerfaces](#) 97 (2012) 162– 170. Towards the understanding of the behavior of single-chained ether phospholipids in model biomembranes: Interactions with phosphatidylethanolamines in Langmuir monolayers)

Three single-chained ether lipids of comparable chemical structure but different biological activities (namely natural platelet activating factor – PAF, its deacetylated precursor – lyso-PAF and synthetic compound – edelfosine – ED) have been investigated in mixed Langmuir monolayers with phosphatidylethanolamines, PEs (DSPE, SOPE and DOPE), serving as model of inner shell of cellular membrane. The aim of undertaken studies was to verify the correlation between minor differences in chemical structures of the investigated ether lipids and their behavior in membrane-mimicking environment. To reach this goal the interactions between particular ether lipids and PEs have been analyzed with  $\pi$ -A values derived from the surface pressure–area isotherms. To get insight into miscibility between film components, Brewster angle microscopy, enabling direct visualization of monolayers structure, has been applied.

Hac-Wydro et al (Katarzyna Hac-Wydro, Roza Lenartowicz, Patrycja Dynarowicz-Łatka, [Colloids and Surfaces B: Biointerfaces](#) 102 (2013) 178– 188. The influence of plant stanol ( $\beta$ -sitostanol) on inner leaflet of human erythrocytes membrane modeled with the Langmuir monolayer technique)

The presence of dietary phytocompounds – plant sterols and stanols – in human plasma and membranes raises the question on their influence on membrane properties. A good way to get an insight into interactions of these biomolecules with membranes at molecular level is to perform experiments on artificial systems, e.g. Langmuir monolayers, composed of membrane lipids. In this paper the influence

of plant stanol –  $\beta$ -sitostanol – on monolayers imitating the inner leaflet of human membrane, composed of phosphatidylethanolamine (POPE)/phosphatidylserine (POPS)/cholesterol (Chol) was studied.

Hac-Wydro et al (Katarzyna Hac-Wydro, Anna Zaja, Patrycja Dynarowicz-Łatka, [Journal of Colloid and Interface Science](#) 360 (2011) 681–689. The influence of plant stanol on phospholipids monolayers – The effect of phospholipid structure)  
This work is aimed at investigating the influence of a plant stanol ( $\beta$ -sitostanol) on Langmuir monolayers from various phospholipids and comparing the effect of

phytostanol versus its unsaturated analog – phytosterol (b-sitosterol). The studied phospholipids differed in the structure of polar head (phosphatidylcholine– PC, phosphatidylethanolamine – PE, phosphatidylserine – PS) as well as in the number of monounsaturated chains in PC molecule.

Jurak and Miñones (Małgorzata Jurak, José Miñones Conde, [Biochimica et Biophysica Acta 1828 \(2013\) 2410–2418](#). Characterization of the binary mixed monolayers of  $\alpha$ -tocopherol with phospholipids at the air-water interface)

The mixed Langmuir monolayers composed of model constituents of biological membranes, 1,2-dipalmitoyl-sn-glycero-3-phosphocholine (DPPC), 2-oleoyl-1-palmitoyl-sn-glycero-3-phosphocholine (POPC), and 1,2-dioleoyl-sn-glycero-3-phosphocholine (DOPC), were investigated to provide information on the intermolecular interactions between these membrane components and the physiologically active vitamin E– $\alpha$ -tocopherol (TF), as well as on the phase behavior of these mixed systems. Additionally, topography of these monolayers transferred onto the mica support was investigated by the inverted metallurgical microscope. Morphological characteristics were directly observed by Brewster angle microscopy (BAM).

Kamo et al (Tomoari Kamo, Tetsurou Handa, Minoru Nakano, [Colloids and Surfaces B: Biointerfaces 104 \(2013\) 128– 132](#). Lateral pressure change on phase transitions of phosphatidylcholine/diolein mixed membranes) investigated the changes in the lateral pressure in mixed membranes of egg yolk phosphatidylcholine (EPC) and a nonlamellar-forming lipid diolein (DO) with respect to increasing DO content. Several fluorescence techniques were employed to probe transitions of EPC/DO lipid mixtures from lamellar to inverted hexagonal via bicontinuous cubic phases.

Ohki et al (Shinpei Ohki, Matthias Müller, Klaus Arnold, Hiroyuki Ohshima, [Colloids and Surfaces B: Biointerfaces 79 \(2010\) 210–218](#). Surface potential of phosphoinositide membranes: Comparison between theory and experiment) studied surface potential of lipid membranes made of phosphatidylcholine (PC) and one of the phosphoinositides (PPI); PI, PIP or PIP<sub>2</sub>, by using the electrophoretic mobility of these lipid membrane vesicles, and a theoretical model of the surface potential developed for these membranes containing PPIs.

Park (Jin-Won Park, [Colloids and Surfaces B: Biointerfaces 71 \(2009\) 128–132](#). Individual leaflet phase effect on nanometer-scale surface properties of phospholipid bilayers)

Phospholipid bilayers were formed on mica using Langmuir–Blodgett technique and liposome fusion, as a model system for biomembranes. Nanometer-scale surface physical properties were quantitatively characterized upon the different phases of the monolayers.

Rey et al (I Rey, J Miñones Jr, P Dynarowicz-Latka, J Miñones, O Conde, *Langmuir* 20 (2004) 11414-11421. Surface behavior of oleoyl palmitoyl phosphatidyl ethanolamine (OPPE) and the characteristics of mixed OPPE-Miltefosine monolayers) investigated monolayers of OPPE and mixed OPPE-Miltefosine using surface pressure-area isotherms and BAM.

Rinia et al (Hilde A. Rinia, Rudy A. Demel, Jan P. J. M. van der Eerden, and Ben de Kruijff, *Biophysical Journal* Volume 77 September 1999 1683–1693. Blistering of Langmuir-Blodgett Bilayers Containing Anionic Phospholipids as Observed by Atomic Force Microscopy) prepared asymmetric bilayers of different phospholipid compositions by the Langmuir-Blodgett (L-B) method, and imaged by atomic force microscopy (AFM). Such bilayers can function as a model for biological membranes. The first leaflet consisted of zwitterionic phospholipids phosphatidylcholine (PC) or phosphatidylethanolamine (PE). The second leaflet consisted of the anionic phospholipid phosphatidylglycerol (PG), in either the condensed or liquid phase or, for comparison, of PC.

Stefaniu and Brezesinski (Cristina Stefaniu and Gerald Brezesinski, *Advances in Colloid and Interface Science* 207 (2014) 265-279. Grazing incidence X-ray diffraction studies of condensed double-chain phospholipid monolayers formed at the soft air/water interface )

The use of highly brilliant synchrotron light sources in the middle of the 1980s for X-ray diffraction has revolutionized the research of condensed monolayers. Since then, monolayers gained popularity as convenient quasi two-dimensional model systems widely used in biophysics and material science. This review focuses on structures observed in onecomponent phospholipid monolayers used as simplified two-dimensional models of biological membranes. In a monolayer system the phase transitions can be easily triggered at constant temperature by increasing the packing density of the lipids by compression. Simultaneously the monolayer structure changes are followed *in situ* by grazing incidence X-ray diffraction. Competing interactions between the different parts of the molecule are responsible for the different monolayer structures. These forces can be modified by chemical variations of the hydrophobic chain region, of the hydrophilic head group region or of the interfacial region between chains and head groups. Modifications of monolayer structures triggered by changes of the chemical structure of double-chain phospholipids are highlighted in this paper.

Szczes et al (A. Szczes, M. Jurak, E. Chibowski, *Journal of Colloid and Interface Science* 372 (2012) 212–216. Stability of binary model membranes—Prediction of the liposome stability by the Langmuir monolayer study)

In this paper, usefulness of the Langmuir monolayer study is demonstrated for predictions of the stability of liposomes composed of dipalmitoyl phosphatidylcholine (DPPC) and cholesterol (Chol). Thermodynamic analysis of the surface pressure (p)–area (A) isotherms of the DPPC/Chol systems was performed, which allowed for concluding on miscibility of the components, their molecular packing, and the interactions between molecules.

Takajo et al (Yuichi Takajo, Hitoshi Matsuki, Hiroki Matsubara, Koji Tsuchiya, Makoto Aratono, Michio Yamanaka, *Colloids and Surfaces B: Biointerfaces* 76 (2010) 571–576. Structural and morphological transition of long-chain phospholipid vesicles induced by mixing with short-chain phospholipid  
Effects of a short-chain phospholipid, dihexanoylphosphatidylcholine (DHPC), on the structure and morphology of membrane assemblies of a long-chain phospholipid, dimyristoylphosphatidylcholine (DMPC), were examined by fluorescence spectroscopy, differential scanning calorimetry (DSC), and cryogenic transmission electron microscopy (cryo-TEM).

Wydro (Paweł Wydro, *Colloids and Surfaces B: Biointerfaces* 106 (2013) 217– 223. The influence of cardiolipin on phosphatidylglycerol/phosphatidylethanolamine monolayers—Studies on ternary films imitating bacterial membranes) studied the properties of ternary systems composed of phosphatidylethanolamines (PEs), phosphatidylglycerols (PGs) and cardiolipin (CL) with the Langmuir monolayer technique and Brewster Angle Microscopy. In all the investigated mixed films the PE:PG = 3:1, which reflects the proportion of these lipids classes in various Gram Negative bacteria. The content of cardiolipin was varied from 5 to 20%, which is in the range of CL concentration in bacterial membranes. The experiments were performed for POPE/POPG/CL and POPE/DPPG/CL films spread on water subphase and on NaCl solution.

Wydro (Paweł Wydro, *Colloids and Surfaces B: Biointerfaces* 103 (2013) 67– 74. The influence of cholesterol on multicomponent Langmuir monolayers imitating outer and inner leaflet of human erythrocyte membrane)  
In this work the Langmuir monolayers were used to prepare multicomponent systems mimicking outer and inner layer of human erythrocyte membranes. The aim of performed experiments was to compare the influence of cholesterol on complex artificial membranes reflecting compositional diversity of the respective membranes leaflets. The properties of both systems in the presence of cholesterol at various concentrations were analyzed by means of thermodynamic description of the interactions between molecules in the investigated monolayers, complemented by the analysis of their morphology performed with the application of Brewster Angle Microscopy

Wydro and Witkowska (Paweł Wydro, Karolina Witkowska, *Colloids and Surfaces B: Biointerfaces* 72 (2009) 32–39. The interactions between phosphatidylglycerol and phosphatidylethanolamines in model bacterial membranes. The effect of the acyl chain length and saturation) applied the Langmuir monolayer technique to study the interactions between phosphatidylglycerol (PG) and phosphatidylethanolamines (PEs). Since the technique of monomolecular layers is useful method of modeling of

biomembranes and the investigated lipids are the major components of Gram-negative bacteria bilayers the results obtained were discussed in the context of the properties of bacterial membranes. To investigate the influence of the phosphatidylethanolamine acyl chain structure on its miscibility and interactions with dipalmitoylphosphatidylglycerol (DPPG) the chosen phosphatidylethanolamines differed both in the length (dipalmitoylphosphatidylethanolamine (DPPE), distearoylphosphatidylethanolamine (DSPE)), and saturation (dioleoylphosphatidylethanolamine (DOPE)) of the hydrocarbon chains.

## Articles d'acid gras-fosfolipid

### Mixed

Eftaiha et al (Ala'a F. Eftaiha, Sophie M.K. Brunet, Matthew F. Paige, [Journal of Colloid and Interface Science](#) 368 (2012) 356–365. Thermodynamic and structural characterization of a mixed perfluorocarbon–phospholipid ternary monolayer surfactant system)

Pulmonary lung surfactant is a mixture of surfactants that reduces surface tension during respiration. Perfluorinated surfactants have potential applications for artificial lung surfactant formulations, but the interactions that exist between these compounds and phospholipids in surfactant monolayer mixtures are poorly understood. We report here, for the first time, a detailed thermodynamic and structural characterization of a minimal pulmonary lung surfactant model system that is based on a ternary phospholipid–perfluorocarbon mixture. Langmuir and Langmuir–Blodgett monolayers of binary and ternary mixtures of the surfactants 1,2-dipalmitoyl-sn-glycero-3-phosphocholine (DPPC), 1,2-dipalmitoyl-sn-glycero-3-phosphoglycerol (DPPG) and perfluorooctadecanoic acid (C18F) have been studied in terms of miscibility, elasticity and film structure. The extent of surfactant miscibility and elasticity has been evaluated via Gibbs excess free energies of mixing and isothermal compressibilities. Film structure has been studied by a combination of atomic force microscopy and fluorescence microscopy.

Gzyl-Malcher and Paluch (Barbara Gzyl-Malcher, Maria Paluch, *Thin Solid Films* 516 (2008) 8865–8872. Studies of lipid interactions in mixed Langmuir monolayers) compared the mixed monolayers of dipalmitoyl phosphatidylcholine (DPPC) with 3-monopalmitoyl glycerol (PG) and palmitic acid 4-methylumbelliferyl ester (4-MU). Relevant thermodynamic parameters such as excess area ( $\Delta A^E$ ) and excess free energy of mixing ( $\Delta G_{\text{mix}}^E$ ) were derived from the surface pressure data obtained from compression measurements performed in a Langmuir trough.

Hac-Wydro and Wydro (K Hac-Wydro and P Wydro, *Chem Phys Lipids* 150 (2007) 66–81. The influence of fatty acids on model cholesterol-phospholipid membranes) verify the influence of the saturated stearic acid and the unsaturated oleic and linolenic fatty acids on model cholesterol/phospholipid membranes. The experiments were based on the Langmuir monolayer technique.



Hac-Wydro et al (Katarzyna Hac-Wydro, Karolina Jedrzejek, Patrycja Dynarowicz-Łatka, *Colloids and Surfaces B: Biointerfaces* 72 (2009) 101–111. Effect of saturation degree on the interactions between fatty acids and phosphatidylcholines in binary and ternary Langmuir monolayers) studied the interactions between fatty acids and phosphatidylcholines in mixed binary and ternary Langmuir monolayers. The compounds investigated, both fatty acids and phospholipids were of the same hydrocarbon chain length and differed in their saturation degree (stearic acid (C18:0)), oleic acid (C18:1), linoleic acid (C18:2) and distearoylphosphatidylcholine—DSPC and dioleoylphosphatidylcholine—DOPC.

He et al (Guangxiao He, Runguang Sun, Changchun Hao, Jing Yang, Man Wang, Lini Zhang, *Colloids and Surfaces A: Physicochem. Eng. Aspects* 441 (2014) 184–194. Thermodynamic analysis and AFM study of the interaction of palmitic acid with DPPE in Langmuir monolayers) studied the influence of PA on 1, 2-dipalmitoyl-sn-glycero-3-phosphoethanolamine (DPPE) monolayer, which is essential to understand those physiological and pathological processes. The behaviors and microstructures of monolayer of PA/DPPE binary systems on subphase of pH 6.2 and 3 were investigated by using a combination of Langmuir technique and Atomic force microscopy (AFM) in this paper. The two kinds of molecular arrangement situations were provided at different molar ratios. The thermodynamic properties of PA /DPPE mixed monolayer have been analyzed quantitatively based on the regular solution theory.

Hao et al (Changchun Hao, Runguang Sun, Jing Zhang, *Colloids and Surfaces B: Biointerfaces* 112 (2013) 441–445. Mixed monolayers of DOPC and palmitic acid at the liquid–air interface) investigated the interactions between 1,2-dioleoyl-sn-glycero-3-phosphocholine (DOPC) and palmitic acid (PA) in mixed monolayers through surface pressure measurements, fluorescence microscopy (FM) and atomic force microscopy (AFM). The miscibility of two components and the interactions between DOPC and PA in the mixed monolayers were accessed by analyzing surface pressure–area isotherms.

Hoda et al (Kazuki Hoda, Hiromichi Nakahara, Shohei Nakamura, Shigemi Nagadome, Gohsuke Sugihara, Norio Yoshino, Osamu Shibata, *Colloids and Surfaces B: Biointerfaces* 47 (2006) 165–175. Langmuir monolayer properties of the fluorinated-hydrogenated hybrid amphiphiles with dipalmitoylphosphatidylcholine (DPPC)) obtained the Surface pressure–area, surface potential–area, and dipole moment–area isotherms for the Langmuir monolayer of two fluorinated-hydrogenated hybrid amphiphiles (sodium phenyl 1-[(4-perfluorohexyl)-phenyl]-1-hexylphosphate (F6PH5PPhNa) and (sodium phenyl 1-[(4-perfluorooctyl)-phenyl]-1-hexylphosphate (F8PH5PPhNa)), DPPC and their two-component systems at the air/water interface. Monolayers spread on 0.02M Tris buffer solution (pH 7.4) with 0.13M NaCl at 298.2K were investigated by the Wilhelmy method, ionizing electrode method and fluorescence microscopy.

Hoda et al (Kazuki Hoda, Hideya Kawasaki, Norio Yoshino, Chien-Hsiang Chang, Yoko Morikawa, Gohsuke Sugihara, Osamu Shibata, *Colloids and Surfaces B: Biointerfaces* 53 (2006) 37–50. Mode of interaction of two fluorinated-hydrogenated

hybrid amphiphiles with dipalmitoylphosphatidylcholine (DPPC) at the air–water interface)

Two-component Langmuir monolayers formed on 0.02M Tris buffer solution (pH 7.4) with 0.13M NaCl at 298.2K were investigated for two different fluorinated-hydrogenated hybrid amphiphiles (F6PH5PPhNa and F8PH5PPhNa or F6 and F8, respectively) with DPPC. Surface pressure ( $\pi$ ), surface potential ( $\Delta V$ ) and dipole moment ( $\mu$ ) as a function of molecular surface area ( $A$ ) were measured by employing the Wilhelmy method and an ionizing electrode method. From the  $A$ – and  $\Delta V$ –XF6 (or XF8) curves, partial molecular surface area (PMA) and apparent partial molecular surface potential (APSP) were determined as a function of surface mole fraction ( $XF_n$ ) at discrete surface pressures. Then, the behavior of occupied surface areas and surface potentials of the respective components could be made clearer. Compressibility ( $C_s$ ), elasticity ( $C_{-1s}$ ), and excess Gibbs energy ( $\Delta G_{ex}$ ) as a function of XF6 (or XF8) were estimated at definite pressures.

Levy et al (MY Levy, S Benita, A Baszkin, Colloids Surf 59 (1991) 225-241. Interactions of a non-ionic surfactant with mixed phospholipid-oleic acid monolayers. Studies under dynamic conditions) performed surface pressure studies of pure and mixed monolayers of phosphatidylcholine, phosphatidylethanolamine, and oleic acid spread at the air–water interface in the presence and in the absence of a non-ionic surfactant in the aqueous subphase.

Mircheva et al (K. Mircheva, M. Gonnet, K. Balashev, Tz. Ivanova, F. Boury, I. Panaiotov, *Colloids and Surfaces A: Physicochem. Eng. Aspects*. Properties of  $\beta$ -carotene and retinoic acid in mixed monolayers with Dipalmitoylphosphatidylcholine (DPPC) and Solutol)

The liposoluble vitamins and carotenoids are sensitive molecules and their antioxidant properties can be dramatically affected when included in membrane environment or in encapsulated carriers as liposomes or lipid nanocapsules (LNCs). The formation and state of mixed monolayers at air-water interface of  $\beta$ -carotene ( $\beta C$ ) or retinoic acid (RA) with dipalmitoylphosphatidylcholine (DPPC) as simplest membrane model or with Solutol (Sol) which forms the soft layer covering the LNCs were studied by means of surface pressure ( $\pi$ ) and surface potential ( $\Delta V$ ) measurements.

Nakahara et al (Hiromichi Nakahara, Shohei Nakamura, Hideya Kawasaki, Osamu Shibata, Colloids and Surfaces B: Biointerfaces 41 (2005) 285–298. Properties of two-component Langmuir monolayer of single chain perfluorinated carboxylic acids with dipalmitoylphosphatidylcholine (DPPC)) obtained The surface pressure– and the surface potential–area isotherms for two-component monolayers of four different perfluorocarboxylic acids (FCns; perfluorododecanoic acid: FC12, perfluorotetradecanoic acid: FC14, perfluorohexadecanoic acid: FC16, perfluorooctadecanoic acid: FC18) with dipalmitoylphosphatidylcholine (DPPC) on subphase solution of 0.15M NaCl (pH 2.0) at 298.2K as a function of compositions in the mixtures by employing the Wilhelmy method, the ionizing electrode method, the fluorescence microscopy, and the atomic force microscopy.



Petelska and Figaszewski (Aneta D. Petelska, Zbigniew A. Figaszewski, *Colloids and Surfaces B: Biointerfaces* 82 (2011) 340–344. The equilibria of phosphatidylcholine–fatty acid and phosphatidylcholine–amine in monolayers at the air/water interface) Monolayers of phosphatidylcholine, fatty acid and amine and binary mixtures phosphatidylcholine–fatty acid or phosphatidylcholine–amine were investigated at the air/water interface. Phosphatidylcholine (lecithin, PC), stearic acid (SA), palmitic acid (PA), decanoic acid (DA) and decylamine (DE) were used to the experiment. The surface tension values of pure and mixed monolayers were used to calculate  $\pi$ –A isotherms.

Torrent Nanobioscience, DPPC-OA. J. Torrent-Burgués *BioNanoSci.* (2011) 1:202–209

Oleamide (OA) and its mixtures with other lipids are of interest in some biological systems, such as the tear film or the cerebrospinal fluid. In this work, the behavior of OA, OA–dipalmitoylphosphatidylcholine (DPPC), and OA–cholesterol films is studied using surface pressure–area isotherms and atomic force microscopy, and analyzing the collapse pressure vs. composition, the compressibility, and the mean area vs. composition for several surface pressures. It is observed that OA forms homogeneous monolayers in a liquid-expanded state until the collapse surface pressure and the mixing with DPPC and cholesterol. The collapse surface pressure changes with the mixture composition, and in the case of DPPC, a noticeable influence of OA in the liquid-expanded/liquid-condensed phase change of DPPC is observed. The excess area is positive for the OA/DPPC films, but mostly negative for the OA–cholesterol films. These results are of interest for the target of formulation of artificial tears containing lipids.

Wydro et al (Katarzyna Hac-Wydro, Karolina Jedrzejek, Patrycja Dynarowicz-Łatka, *Colloids and Surfaces B: Biointerfaces* 72 (2009) 101–111. Effect of saturation degree on the interactions between fatty acids and phosphatidylcholines in binary and ternary Langmuir monolayers) studied in this work the interactions between fatty acids and phosphatidylcholines were in mixed binary and ternary Langmuir monolayers. The compounds investigated, both fatty acids and phospholipids were of the same hydrocarbon chain length and differed in their saturation degree (stearic acid (C18:0)), oleic acid (C18:1)), linoleic acid (C18:2) and distearoylphosphatidylcholine—DSPC and dioleoylphosphatidylcholine—DOPC).